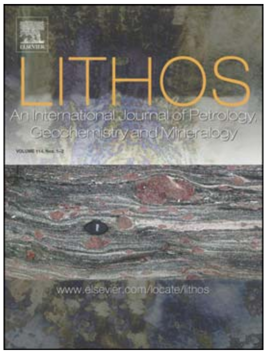

The basaltic volcanism of the Dumisseau Formation in the Sierra de Bahoruco, SW Dominican Republic: A record of the mantle plume-related magmatism of the Caribbean Large Igneous Province

Javier Escuder-Viruete, Marc Joubert, Manuel Abad, Fernando Pérez-Valera, Janet Gabites

PII: S0024-4937(16)30004-4
DOI: doi: 10.1016/j.lithos.2016.03.013
Reference: LITHOS 3873

To appear in: *LITHOS*

Received date: 7 November 2015
Accepted date: 14 March 2016

Please cite this article as: Escuder-Viruete, Javier, Joubert, Marc, Abad, Manuel, Pérez-Valera, Fernando, Gabites, Janet, The basaltic volcanism of the Dumisseau Formation in the Sierra de Bahoruco, SW Dominican Republic: A record of the mantle plume-related magmatism of the Caribbean Large Igneous Province, ***LITHOS*** (2016), doi: 10.1016/j.lithos.2016.03.013

The basaltic volcanism of the Dumisseau Formation in the Sierra de Bahoruco, SW Dominican Republic: a record of the mantle plume-related magmatism of the Caribbean Large Igneous Province

Javier Escuder-Viruete[1,*], Marc Joubert[2], Manuel Abad[3],
Fernando Pérez-Valera[4], Janet Gabites[5]

[1]Instituto Geológico y Minero de España, C. La Calera 1, 28760 Tres Cantos, Madrid. Spain. j.escuder@igme.es

[2] BRGM. Av. C. Guillemin. 45060 Orléans. France. m.joubert@brgm.fr

[3] Departamento de Geología. Universidad de Atacama. Av. Copayapu 485, Copiapó, Chile. manuel.abad@uda.cl

[4] Centro de Estudios Avanzados en Ciencias de la Tierra-Universidad de Jaén, Campus Las Lagunillas s/n, 23071 Jaén, Spain. fperez@ujaen.es

[5] Pacific Centre for Isotopic and Geochemical Research. University of British Columbia, 6339 Stores Road Vancouver, BC V6T-1Z4. Canada. jgabites@eos.ubc.ca

Abstract

The basaltic volcanism of the Dumisseau Fm in the Sierra de Bahoruco, SW Dominican Republic, offers the opportunity to study, on land, the volcanism of the Caribbean Large Igneous Province (CLIP). It consists of an at least 1.5 km-thick sequence of submarine basaltic flows and pyroclastic deposits, intruded by doleritic dykes and sills. Three geochemical groups have been identified: low-Ti tholeiites (group I); high-Ti transitional basalts (group II); and high-Ti and LREE-enriched alkaline basalts (group III). These geochemical signatures indicate a plume source for all groups of basalts, which are compositionally similar to the volcanic rocks that make up various CLIP fragments in the northern region of the Caribbean Plate. Trace element modelling indicates that group I magmas are products of 8-20% melting of spinel lherzolite, group II magmas result 4-10% melting of a mixture of spinel and garnet lherzolite, and group III basalts are derived by low degrees

(0.05-4%) of melting of garnet lherzolite. Dynamic melting models suggest that basalts represent aggregate melts produced by progressive decompression melting in a mantle plume. There is no compositional evidence for the involvement of a Caribbean supra-subduction zone mantle or crust in the generation of the basalts. Two $^{40}Ar/^{39}Ar$ whole-rock ages reflect the crystallization of group II magmas at least in the late Campanian (~74 Ma) and the lower Eocene (~53 Ma). All data suggest that the Dumisseau Fm is an emerged fragment of the CLIP, which continues southward through the Beata Ridge

(*) Corresponding Author

Key words: oceanic plateau basalts; Dumisseau Formation; mantle plume magmatism; Caribbean Large Igneous Province; Dominican Republic

1. Introduction

Much of the Caribbean Plate is widely interpreted as an oceanic plateau, or a Caribbean large igneous province (CLIP), that formed by by the emplacement of mafic magmas above a mantle plume (e.g., Kerr et al., 1997, 2003). The huge amount of generated melt has led to the formation of anomalously thick oceanic crust (15-20 km) which characterises the province in the Caribbean basin (Donnelly et al., 1990; Donnelly, 1994; Mauffret and Leroy, 1997; Diebold et al., 1999). Petrological, geochemical and isotopic studies of the uplifted and tectonically accreted sections of the CLIP, around the margins of the Caribbean plate, are also consistent with this interpretation (e.g., Hauff et al., 2000; Kerr et al., 1997, 2002, 2009; Sinton et al., 1998; Lapierre et al., 1997, 2000; Kerr and Mahoney, 2007; Jolly et al., 2007; Escuder-Viruete et al., 2007, 2010, 2011a). These studies have resulted in several geodynamic models for the origin and evolution of the CLIP (Montgomery et al., 1994; Pindell et al., 2005; Hastie and Kerr, 2010; Pindell and Kennan, 2009; Wright and Wyld, 2011; Loewen et al., 2013; Whattam and Stern, 2015). However, there are several key issues that remain to be resolved and need to be incorporated in any proposed geodynamic model for the CLIP. These include its volcanic stratigraphy, the sequence and age of successive plume-related melting events, the significant geochemical and isotopic homogeneity of the resulting mafic melts, and the spatial and temporal relationships with subduction events around the Caribbean.

In this paper, the basaltic volcanism of the Dumisseau Formation (DFm) is studied. The DFm constitutes the Cretaceous igneous basement of the Massif de la Hotte and the Chaîne de la Serre in Haiti, the Sierra de Bahoruco in SW Dominican Republic, and probably the submarine promontory of the Beata Ridge (Figs. 1, 2). All these areas have been grouped as a geological terrain and interpreted as a fragment of the CLIP, uplifted/accreted on the northern margin of the Caribbean Plate (Sen et al., 1988; Lewis and Draper, 1990; Mann et al., 1991; Sinton et al., 1998; Révillon et al., 2000). The new field, petrologic, geochemical and geochronological data of the DFm presented in this paper allows us to establish the nature of the magma sources and the mantle melting conditions, as well as the magmatic history of the region. Additionally, our results allow the correlation of the DFm with other contemporaneous volcanic units of the CLIP and help in the formulation of a tectonomagmatic evolutionary model for the northern Caribbean plate during the late Cretaceous.

2. Geological Context

2.1. The Caribbean Large Igneous Province (CLIP)

The CLIP is generally believed to have formed by the eruption of a huge volume of mafic magmas derived from a mantle plume onto what would become the oceanic Caribbean plate (Duncan and Hargraves, 1984; Kerr et al, 1997, 2002, 2003; Sinton et al, 1998; Hauff et al., 2000). The submerged part of the plateau has been sampled at the Beata Ridge and DSDP Leg 15 and 165 ODP Leg sites (Fig. 1; Donnelly et al., 1990; Sinton et al., 1998; Révillon et al., 2000; Kerr et al., 2009), but it also outcrops on land in Jamaica, central and southern Hispaniola (Dominican Republic and Haiti), SW Puerto Rico, coastal borders of Venezuela, Curacao and Aruba, the Pacific coast of Central America (Costa Rica and Panama), and western Colombia and Ecuador (Buchs et al, 2010; Escuder-Viruete et al., 2007, 2011; Hastie and Kerr, 2010; Hastie et al, 2008, 2009; Hauff et al., 2000; Kerr et al, 1997, 2002; Lapierre et al., 2000; Lewis et al., 2002; Montes et al., 2012). In its northern part, the CLIP was built in three phases: 124-112 Ma (Lapierre et al, 2000; Escuder-Viruete et al., 2007), 94-83 Ma (apparently the most voluminous, Kerr et al., 1997, 2002; Sinton et al., 1998; Hastie et al., 2008, 2009; Loewen et al., 2013), and 80-68 Ma (Révillon et al., 2000; Escuder-Viruete et al., 2011a; Sandoval et al., 2015). Recently, Whattam and Stern (2015) have compiled radiometric ages in Central American and NW South American, and concluded that CLIP plume activity mainly occurred between 92 and 88 Ma with two less frequent magmatic pulses at 124-112 Ma and 76-72 Ma. Thus, rather than a single event at ~90 Ma as it was initially proposed, the CLIP magmatism occurred from the Aptian to the Maastrichtian, peaking around the Turonian-Conacian boundary. These phases have been recognised also in Costa Rica (Hauff et al., 2000; Hoernle et al., 2004) and in other Pacific oceanic plateaus (Kerr, 2003), where the plume magmatism took place intermittently over tens of Ma. Although the CLIP encompasses a wide range of mafic and ultramafic compositions, most of the lavas have a flat or slightly LREE enriched chondrite-normalised REE patterns and ε_{Nd} values between +8.5 and +6.0 (Sinton et al., 1998; Hauff et al., 2000; Lapierre et al., 2000; Révillon et al., 2000; Kerr, 2003; Thompson et al., 2004; Jolly et al., 2007; Escuder-Viruete et al., 2008, 2011a; Lowen et al., 2013).

A Pacific provenance for the CLIP is generally accepted (e.g., Pindell et al., 2005; Mann et al., 1991, 2007; Bandini et al., 2011; Buchs et al., 2010), because the Caribbean oceanic crust includes radiolarites of Pacific affinity at various locations, as in Désiderade, Hispaniola and Puerto Rico (Montgomery et al., 1994; Montgomery and Pessagno, 1999; Baumgartner et al, 2008; Montgomery and Kerr, 2009; Escuder-Viruete et al., 2010; Bandini et al., 2011; Sandoval et al., 2015). Plate tectonic models suggests that the eastern movement of the Farallon plate in the Cretaceous-Paleogene transported the CLIP towards the proto-Caribbean oceanic domain, that had opened by divergence between North and South America from the Jurassic (Pindell et al, 2005; Mann et al., 2007; Flores, 2009; Pindell and Kennan, 2009). However, the geodynamic cause of this eastern movement is unclear, especially from the time of the start of subduction below the Costa Rica-Panama arc about 75 Ma ago (late Campanian; Buchs et al., 2010).

The volcanic stratigraphy of the CLIP is only partially known. In the Caribbean basin, the upper limit of the CLIP lavas has been identified seismically as the basement surface B", which is located under the reflector A" of sedimentary rocks of Eocene age (Mauffret and Leroy, 1997; Driscoll and Diebold, 1999). This B" boundary has been drilled at five locations of DSDP and ODP Sites, where the appearance below of basalts support the occurrence of a single volcanic province in the Caribbean (Sinton et al., 1998). The basalts at the site 151 yielded K-Ar ages of 85-83 Ma (Donnelly et al., 1990), the basaltic sill drilled at the site 152 intrudes Campanian sediments (83-70 Ma) and the basalts of site 1001 have ^{40}Ar-^{39}Ar ages of ~81 Ma (Sinton et al., 2000). These basalts are therefore younger than the ~90 Ma main phase of the CLIP and appear to be part of a separate phase, which possibly related to late rifting in the Caribbean plate (Sinton et al., 1998). Samples recovered in the Beata Ridge include gabbro, dolerite and rare pillow basalt (Révillon et al., 2000), which have a trace elements and isotopic signatures similar to CLIP basalts. Eight samples have ^{40}Ar-^{39}Ar ages between 80 and 75 Ma, but there are also two younger ages of ~55 Ma. Loewen et al. (2013) present new ^{40}Ar-^{39}Ar ages for the Dumisseau Fm in Haiti and the Curaçao Lava Fm, which appears to show that CLIP volcanism was active from 94 to 63 Ma.

2.2. Geodynamic models for the origin of the CLIP

Using petrological, seismic or geodynamic data, various models have been proposed for the generation of the CLIP (Diebold et al., 1999; Driscoll and Diebold, 1999; Mauffret and Leroy, 1999; Kerr et al., 2003; Pindell et al., 2005; Mann et al., 2007; Flores, 2009; James, 2009; Pindell and Kennan, 2009; Hastie and Kerr, 2010; Wright and Wyld, 2011; among others). Placed in the context of the geodynamic evolution of the “Great Arc” of the Antilles, the models for a Pacific-derived origin of the CLIP can be grouped in two end-members. In the first group, the “Great Arc” develops above an east-dipping subduction zone in the Early Cretaceous. The CLIP mostly forms at ~90 Ma on the Farallon Plate which is subducting beneath the east-facing “Great Arc”. When the thick CLIP crust collided with the “Great Arc” in the Late Cretaceous (~85–80 Ma), subduction reversal occurred and arc volcanism is renewed above a west-dipping subduction zone (e.g., Kerr et al., 2003; Hastie and Kerr, 2010). In the second group of models, subduction reversal occurs in the Aptian (~120 Ma), prior to formation of the CLIP, and the later (<120 Ma) magmatism in the “Great Arc” occurs above a west-dipping subduction zone. The CLIP forms in the upper Caribbean Plate of this subduction zone at ~90 Ma and does not collide with the arc (e.g., Pindell et al., 2006).

For the northern margin of the Caribbean plate, Escuder-Viruete et al. (2011b, 2013) proposed a tectonomagmatic model for the generation of the young (78-69 Ma) non-arc-like volcanic rocks outcropping in the Cordillera Central of Hispaniola. In this model, the volcanic rocks were not generated from a late-stage pulsing of the Caribbean plume, but through unrelated and spatially distinct mantle-melting events controlled by a plate-scale mechanism that sampled a similar mantle source material. The SW-directed subduction of the proto-Caribbean slab drives rollback and migration of the overlying Caribbean island-arc toward the NE. To balance the rollback, mantle influenced by the Caribbean plume was advected into the mantle wedge below the extended island-arc. The upwelling of this enriched mantle toward the Caribbean back-arc spreading centre produced relatively enriched MORB-type magmas in the NE sector of Cordillera Central (DC and SC in Fig.

1), and off-axis OIB-type magmas in the SW sector (BPP in Fig. 1). This model has been extended to the Lesser Antilles and Central America subduction zones in the late Cretaceous by Loewen et al. (2013), where the slab rollback created an extensional regime within the overlying Caribbean plate. Following these authors, mixing of plume with upwelling asthenospheric mantle in the back-arc areas provided a source for intermittent melting and eruption through the original plateau over a 30 Ma period. On the basis of geochemical and chronological data, Whattam and Stern (2015) propose a late Cretaceous tectonic evolution of Central America, NW South America and the Leeward Antilles consistent with a plume-induced subduction initiation at 95 Ma along the southern and western margins of the CLIP.

2.3. Basaltic units related to the CLIP in Hispaniola

In Hispaniola, the basaltic units with oceanic plateau affinities include the Dumisseau Fm of southern Haiti (Sen et al., 1988) and SW Dominican Republic (this work, Fig. 1), the Duarte Complex, the Siete Cabezas Fm and the Pelona-Pico Duarte Fm of the Cordillera Central. All these basalts have been interpreted as partial melts of a mantle plume source, which has not been contaminated by subduction (Escuder-Viruete et al., 2007, 2011). In the Chaîne de la Serre, the DFm consists of massive and pillowed basalts with subordinate picrites, interlayered with pelagic limestone, volcanogenic and biogenic turbidites, cherts and shales (Maurrasse et al., 1979). These authors distinguish two sections of upper and lower basalts, in which the fossil content in the interbedded sediments indicates an Early Cretaceous to Santonian age and an upper Campanian age, respectively. Sinton et al. (1998) obtained two ^{40}Ar-^{39}Ar plateau ages of 88.7±1.5 and 92.0±4.8 Ma for the lower basalts and Sen et al. (1988) report a K-Ar age of 75.0 ± 1.5 Ma for a sill in the upper basalts. Maurrasse et al. (1979) describe an erosional unconformity on top of the DFm that marks the end of volcanism in the Chaîne de la Serre. Overlying the unconformity a basal conglomerate of basaltic clasts, sandstones and pelagic limestones of latest Maastrichtian to early Paleocene age occurs (Beloc Fm; Maurrasse et al., 1979), but in other areas the sequence is composed of limestones of upper Campanian to Maastrichtian age. In the Massif de la Hotte, Calmus (1983) describes a similar stratigraphic relationship, in which lower Paleocene conglomerates unconformably overlie pelagic limestones, cherts and basalts of the late Cretaceous Macaya Fm. In the Sierra de Bahoruco, van den Berghe (1983) reported Maastrichtian basalts unconformably overlain by Paleocene-Eocene limestones. In summary, the basaltic magmatism of the DFm in the whole area of Hotte-Selle-Bahoruco ended before the Paleocene.

In the Cordillera Central, the Duarte Complex comprises a ~3 km-thick sequence of mafic and ultramafic meta-volcanic rocks, heterogeneously deformed and metamorphosed, intruded by arc-related batholiths of late Cretaceous age (91-83 Ma; Lewis et al., 2002; Escuder-Viruete et al., 2007, 2010). The complex includes clinopyroxene-bearing porphyritic metapicrites and Mg-rich metabasalts, geochemically similar to the more enriched CLIP lavas (Lapierre et al., 1997, 2000; Escuder-Viruete et al., 2007). ^{40}Ar-^{39}Ar plateau ages of metamorphic hornblende indicate a pre-Cenomanian age (probably Albian) for the first phase of the CLIP volcanism. The Siete Cabezas Fm consists of massive and pillowed basalt, subordinate pyroclastic breccias, vitric tuffs and cherts (Donelly et al., 1990), which unconformably overlain the Duarte Complex (Escuder-Viruete et al., 2008). Radiolarians included in sediments have provided a middle Campanian to Maastrichtian age (Montgomery and Pessagno, 1999; Sandoval et al., 2015). Sinton et al. (1998) obtained consistent Maastrichtian Ar-Ar ages. These ages and the geochemical characteristics of the lavas (tholeiitic basalts with flat REE patterns) are consistent with a CLIP origin (Sinton et al., 1988; Lewis et al., 2002; Escuder-Viruete et al., 2008). The Pelona-Pico Duarte Fm is composed of a 1.5-3 km-thick sequence of basalts of transitional tholeiitic and alkaline compositions (Escuder Viruete et al., 2011). Basalts are rich in TiO_2 and Nb, with a marked LREE enrichment and HREE depletion, and have a very restricted range of $(\varepsilon_{Nd})_{70\ Ma}$ values between +5.0 and +5.9. These characteristics are similar to the enriched basalts of the CLIP (Kerr et al., 1997, 2002, 2009), particularly to those found at DSDP site 152 and the Beata Ridge. ^{40}Ar-^{39}Ar data indicate a middle Campanian-Maastrichtian age for magmatism, correlating with the late phase of CLIP volcanism (Escuder Viruete et al., 2011).

3. The Dumisseau Formation in the Sierra de Bahoruco

3.1. Field relations and petrography

The outcrops of the DFm in the Sierra de Bahoruco are located in the core of km-scale, NW-SE-trending anticlines, generally occupying topographically depressed areas, and in the eastern coastal area, where a NNE-SSW-trending normal fault cuts and sinks under the Caribbean Sea the mountainous alignement (Figs. 1, 2; Llinás, 1972; De León, 1989; Abad, 2010; Joubert, 2010; Pérez-Valera, 2010). The DFm consists of at an least 1.5 km-thick sequence of basaltic flows and pyroclastic deposits, minor volcanogenic sedimentary deposits, and intrusions of doleritic dykes and sills (Escuder-Viruete, 2010). No felsic volcanic products have been observed. Following the terminology of McPhie et al. (1993), three types of volcanic facies have been distinguished: (1) coherent mafic flows and monogenic autoclastic breccias resulting effusive processes; (2) mafic breccias and tuffs formed by subaqueous explosive eruptions; and (3) re-sedimented syn-eruptive polygenetic breccias and fine-grained volcaniclastic deposits. Basaltic flows (<10 m-thick) are blue-grey to brown, with massive, flow-foliated or pillowed structures. They exhibit porphyritic, microporphyritic, aphanitic, glassy and amygdaloidal textures. The related feeder dykes have massive or flow-foliated structures. They exhibit intergranular and ophitic textures. The amygdaloidal facies present vacuoles filled with quartz, calcite and zeolites. The mafic pyroclastic deposits are complosed of lithic clast-rich breccias and fine-grained lithic and vitreous tuffs, often with graded and laminated internal structure. The volcaniclastic deposits consist of re-sedimented breccias of centimetre-size polygenetic clasts and fine-grained deposits. Interbedded sediments are rare and consist of lenses of pelagic limestone and chert. These materials are unconformably overlain by red-algae limestones of middle Eocene age (Pérez-Valera y Abad, 2010).

The main petrographic types observed in the DFm (Fig. 2) are olivine basalts, clinopyroxene (Ti-rich augite) basalts, ortho and clinopyroxene basalts, plagioclase and clinopyroxene basalts, plagioclase basaltic andesites and aphanitic basalts (Escuder-Viruete, 2010). Olivine basalts display a microglomero to microporphyritic texture with an intersectal to subophitic groundmass. The olivine microphenocrysts (<10% modal) are bipyramidal or skeletal, in a matrix formed by an aggregate of plagioclase, ortho and clinopyroxene. Clinopyroxene basalts are the predominant lithology in the DFm. In the porphyritic facies, ortho and clinopyroxene are idiomorphic and milimetric in size. The high modal abundance of clinopyroxene and presence of reaction rims in some samples suggests that they are cumulate phases. The matrix also includes plagioclase, olivine, Fe-Ti spinel, ilmenite and magnetite. In the plagioclase and clinopyroxene basalts the amygdale concentration in horizons often defines a flow banding. These rocks are characterised by plagioclase phenocrysts (<20% modal; 1-2 mm in size) with ophitic and trachytic textures. The andesitic basalts typically exhibit plagioclase phenocrysts (<1 cm length) in a fluidal groundmass rich in microprisms of the same mineral (<45% modal). The aphanitic basalts are commonly vesicular and consist of aligned plagioclase grains (<0.5 mm length, 0-15% modal) in a micro and cryptocrystalline matrix composed of plagioclase, clinopyroxene and magnetite. In the amygdaloidal facies, the vesicles are 0.5-10 mm in diameter, and are filled with calcite, quartz, chlorite, pumpellyte, albite, prenhite, yellow epidote and cryptocrystalline material.

The intrusive rocks of the DFm comprise ortho and clinopyroxene dolerites, clinopyroxene dolerites, microgabbros and ferrodolerites. Petrographically, the ortho and clinopyroxene dolerites are composed of a framework of medium-to-fine grained plagioclase prisms, encompassed by large clinopyroxene poikilitic grains, with interstitial orthopyroxene and skeletal magnetite. In the clinopyroxene dolerites, plagioclase forms intergrowths of large sub-idiomorphic prisms, which host small acicular prisms of clino and orthopyroxene. The ferrodolerites consist of interlocking plagioclase microphenocrysts, clinopyroxene aggregates and abundant skeletal grains of magnetite.

Macroscopically, the monogenetic auto-breccias have a dark reddish-brown colour and are markedly heterogranular. They are composed by angular to sub-rounded lithic clasts of similar basalt (<15 cm), cemented by quartz and calcite. The polygenetic breccias and microbreccias are composed of sub-angular lithic clasts of basaltic nature (>65%), fragments of plagioclase, ortho and clinopyroxene crystals (<15%), or their pseudomorphs, and silicified/palagonitised glass (<20%) in a sparse micro- to cryptocrystalline matrix (<5%), cemented by quartz and calcite. The lithic fragments have fluidal, microporphyritic, aphanitic and doleritic textures. Tuffs deposits are brown to green in colour and are composed of fine-to-coarse-grained, angular to sub-angular fragments of basalt. Under the microscope, the fragments are of glassy and scoriaceous nature (>90%), containing "Y"-shaped spicules and triple points, often crushed and deformed, suggesting a still hot deposition. They also include fragmented pseudomorphs (<5%) of clinopyroxene and plagioclase.

3.2. Post-magmatic alteration

All volcanic facies are affected by a post-magmatic hydrothermal alteration, usually accompanied by a static mineral replacement (Fig. 3). It produces a variable growth of prenhite, pumpellyte, albite, chlorite, brown mica, sericite, white mica, calcite, yellow epidote and Fe-oxides, which form poikilitic and pseudomorphic textures. They indicate zeolite, prenhite-pumpellyte and low-T greenschist facies metamorphism. This hydrothermal alteration is often associated with a network of veins and patches, millimetre-to-centimetre-thick, filled by a white-blue aggregate of carbonates, zeolites and pectolite (larimar). A supergene alteration is variably superimposed and characterised by a red staining of the rocks by Fe oxides.

4. ^{40}Ar/^{39}Ar Geochronology

Two samples of the DFm were selected for ^{40}Ar/^{39}Ar analysis (Fig. 4) with the aim of dating the cooling ages of the magmas. The methodology and the complete data set of the incremental heating ^{40}Ar-^{39}Ar experiments are included in Appendix A and B. All ages are quoted at the 2σ level of uncertainty. Sample 5969I-JE9623 is a very high-Ti-Nb aphyric basalt, of transitional affinity, from the Enriquillo sector. For ten steps (1-10), the obtained plateau age from whole rock is 74.2±1.7 Ma representing 99.6% of the ^{39}Ar released. Therefore, the DFm includes basalts erupted in the late Campanian (age scale of Gradstein et al., 2012). Sample 5970II-MJ9150 consists of a fresh, unfractionated (Mg#=56) dolerite dyke intrusive in pervasively altered basalts, located on the coast road south to Bahoruco. Ti and Nb contents, as well as other geochemical characteristics, are typical of transitional basalts (Appendix C). For nine steps (1-9), the obtained plateau age of whole-rock is 52.8±1.7 Ma for 99.9% of the ^{39}Ar released. A magmatic event of lower Eocene age therefore exists in the Sierra of Bahoruco, which post-dates the hydrothermal alteration processes.

5. Geochemistry

5.1. Chemical changes due to alteration and metamorphism

The analytical techniques and methods used to obtain the bulk-rock composition of samples of the DFm are described in Appendix A. The analytical results, including data of the accuracy and reproducibility, are included in Appendix C. The analysed basalts have been variably altered and metamorphosed from zeolite to greenschist facies conditions. Major (e.g., Si, Na, K, Ca) and trace (e.g., Cs, Rb, Ba, Sr) element contents may have been therefore mobilised by low-T alteration processes. However, the HFSE (Y, Zr, Hf, Ti, Nb and Ta), REE, transition elements (V, Cr, Ni and Sc) and Th, are generally unchanged under a wide range of metamorphic conditions, including seafloor alteration at low to moderate water/rock ratios (Bienvenu et al., 1990). In this work, the geochemical characterization of the DFm and the petrogenetic discussion will be based mostly on the

HFSE and REE, as it can be assumed that they were not significantly affected by alteration or metamorphism. The good correlation obtained when Zr is plotted against Th, Nb, La, Sm, Ti and Yb further confirms that these elements are relatively immobile, and the differences that arise are due to varying degrees of partial melting, differences in the mantle source or the result of magmatic differentiation.

5.2. Major and trace element compositions

The geochemical characteristics of the DFm in the Sierra de Bahoruco are presented in Figs. 5, 6 and 7. As evidenced by the low SiO_2 and K_2O contents, and high values of loss on ignition (LOI>4 wt.%), these volcanic experienced a variable degree of hydrothermal alteration. For a restricted range in SiO_2 (46.5-48.6 wt.%), and excluding the obviously altered samples, the basaltic rocks have relatively high alkali, TiO_2, P_2O_5 and Fe_2O_{3T} contents, for relative low CaO and Al_2O_3 contents (Appendix C). On the basis of MgO contents (Fig. 6), samples can be classified as tholeiitic (<8 wt.%) and high-Mg basalts (8-12 wt.% MgO). Picritic compositions are probably represented by pyroxene-rich cumulate lavas, which were not analysed. In a N-MORB-normalised multi-element plot (Fig. 7), the samples have LREE enriched ($[La/Nd]_N$=0.8-3.4) and depleted HREE ($[Sm/Yb]_N$=0.8-6.5) patterns, with moderate to very high Nb contents (2.8-162 ppm). They do not have positive Pb, K and Sr spikes, and negative Nb-Ta anomalies, typical of subduction-related rocks. However, some samples have a selective enrichment in Rb, Ba and U, as well as a strong depletion in K, which probably results from seafloor hydrothermal alteration. The slight positive Ti anomaly present in some evolved basalts can be related to Fe-Ti oxide accumulation.

Based on the TiO_2 content, multi-element pattern and values of incompatible trace elements ratios, three geochemical groups can be identified in the DFm: low-Ti tholeiites (group I); high-Ti or transitional basalts (group II); and high-Ti and LREE-enriched alkaline basalts (group III). Group I magmas also occur as dykes in the basalts of groups II and III. The lower degree of hydrothermal alteration of group I rocks is also consistent with them being younger.

Low-Ti tholeiites (group I). This group is represented by basaltic flows and microgabbroic/doleritic dykes, which have primitive or slightly fractionated magma compositions (Mg#=66-49). For relatively high MgO contents, the TiO_2, Zr and Nb contents are low (Appendix C). They have high Cr and Ni contents and Th concentrations are relatively low. The Nb/Y values are typical of tholeiitic magmas. In a primitive mantle (N) extended REE diagram, they are characterised by flat patterns ($[La/Yb]_N$=0.7-1.2; Fig. 8a), without fractionation of LREE ($[La/Nd]_N$=0.8-1.0) and HREE ($[Sm/Yb]_N$=0.8-1.2), minor positive anomalies in Nb (relative to Th and La, Nb*=1.1-1.8; where Nb*=0,3618*Nb/(Th*La)^0,5), and no negative Zr-Hf anomaly.

High-Ti transitional basalts (group II). This group is represented by transitional basaltic lavas, which have slightly fractionated compositions (Mg#=57-52). For similar ranges of MgO, the TiO_2, Zr, and Nb contents are higher than those of group I. Cr, Ni and Th contents are also comparatively high. Nb/Y values are typical of transitional magmas. They have extended REE patterns (Fig. 8b) characterised by flat LREE ($[La/Nd]_N$=1.1-1.3), HREE depletion ($[Sm/Yb]_N$=2.4-2.6), and slightly positive anomalies in Nb (Nb*=1.3-1.7).

High-Ti and LREE-enriched alkaline basalts (group III). The group includes olivine, clinopyroxene and plagioclase-phyric basalts, which have moderately fractionated compositions (Mg#=52-45). For the highest TiO_2 contents, the group III lavas are also enriched in Fe. The CaO contents are high, which may be due to the plagioclase accumulation in the magmas and/or to carbonation processes during the late alteration, as suggested by the high-LOI values. The Nb/Y values are typical of alkali magmas. For lower MgO contents, the Zr and Nb concentrations are higher than in groups I and II.

Cr and Ni values are relatively low and indicate advanced fractionation of the magmas. Th contents are the highest found in the DFm. The group III samples have extended REE patterns with extreme negative slopes ($[La/Yb]_N$=25-59; Fig. 8c). Compared with the group II samples, these basalts have a marked LREE enrichment ($[La/Nd]_N$=2.6-3.4) and a greater depletion in HREE ($[Sm/Yb]_N$=4.0-7.3). They show very slight positive anomalies in Nb (Nb*=1.0-1.8), Eu or Ti, but distinct negative Zr-Hf anomalies (Fig. 8c).

6. Interpretation

6.1. Magmatic context of the Dumisseau Fm

The DFm in the Sierra de Bahoruco consists of a >1.5 km-thick sequence of volcanic rocks of essentially basaltic composition. The presence of pillow-lavas with quench textures, the rare interbedded lenses of chert and pelagic limestone, and the nature and pervasive character of the hydrothermal alteration indicate that all volcanic facies were erupted in a relatively deep marine environment. The mineral assemblages of the prenhite-pumpellyte to low-T greenschist facies and the pseudomorphic replacement textures produced during the alteration are typical of a seafloor hydrothermal metamorphism. No evidence of subaerial eruptions has been found. The prevalence of subaqueous lava facies, the high effusive rates deducted by the scarcity of intercalated sediments, the almost exclusively basaltic compositions, and the trace-elements contents and ratios, suggest that the DFm is the result of an oceanic intraplate magmatism produced by high melting rates induced by a mantle plume (e.g., Kerr, 2003). The DFm experienced uplift and was unconformably covered by shallow, red-algae limestones in the middle Eocene (Pérez-Valera and Abad, 2010)

6.2. Age of the Dumisseau Fm in the Sierra de Bahoruco

The $^{40}Ar/^{39}Ar$ age obtained for basalt 5969I-JE9623 indicates extrusive activity at least during the late Campanian (~74 Ma). The age of ~53Ma obtained in the unaltered dyke 5970II-MJ9150 indicates the formation of transitional magmas until the lower Eocene. As this dyke intrudes basalts the affected by the pervasive hydrothermal alteration, this last process is probably pre-lower Eocene. The Fig. 4c includes stratigraphic columns and ^{40}Ar-^{39}Ar ages for the CLIP units in Hispaniola as well as other relevant areas, which allow us to correlate magmatic events along the northern edge of the Caribbean plate. As shown, the basalts of the DFm in the Sierra de Bahoruco are similar in age to those of the upper basalts of the DFm in Haiti (Sen et al., 1988), confirming their correlation. The basalts of the Pelona-Pico Duarte Fm in the Cordillera Central have yielded ^{40}Ar-^{39}Ar ages of 79-68 Ma (middle Campanian to Maastrichtian; Escuder-Viruete et al., 2011a) also result from a similar event. The basalts of the Siete Cabezas Fm in the eastern Cordillera Central also belong to this event, as they have yielded ^{40}Ar-^{39}Ar ages of 69-68 Ma (Sinton et al., 1998) and contain intercalated radiolarites of middle Campanian to Maastrichtian age (Montgomery and Pessagno, 1999). These ages are similar to those of the Nb-rich mafic lavas of the Sabana Grande Fm in SW Puerto Rico (Campanian; Jolly et al., 2007) and the main magmatic activity recorded in the Beata Ridge (80-75 Ma; Révillon et al. 2000), all attributed to the CLIP. Temporarily, this Campanian magmatism may be correlated to the third phase of the CLIP construction of Kerr et al. (2002), as well as with part of oceanic complexes of the Pacific coast of Costa Rica (Hauffet al., 2000; Hoernle et al., 2004; Denyer et al., 2006). However, these relationships do not rule out that the DFm in the Sierra de Bahoruco also contains older volcanic rocks of the CLIP.

On the Beata Ridge 55-53 Ma gabbros and dolerites have been dated by Révillon et al. (2000). As in the case of the dyke of the DFm intruded at ~53Ma, these younger magmas are geochemically and isotopically similar to the older mafic rocks (80-75 Ma), providing evidence of a long magmatic activity in the CLIP. To account for the several magmatic phases over time in the Beata Ridge and Cordillera Central in Hispaniola, Révillon et al. (2000) and Escuder-Viruete et al. (2011) propose that melting could be due to geodynamic processes unrelated to mantle plumes, such as late lithosphere thinning in the Caribbean Plate and adiabatic melting of upwelling enriched mantle. Révillon et al. (2000), proposed that the 55-53 Ma phase had an extensional origin localised in the Beata Ridge. These extensional tectonics may also affect its northern extension in the Sierra of Bahoruco.

6.3. Geochemical diversity of the Dumisseau Fm

Taken together, the Mg# values of 66-47 indicate that the mafic magmas of the DFm experienced low to moderate amounts of fractionation. The basalts show an increase of SiO_2, TiO_2, Fe_2O_3, CaO, Al_2O_3, alkalis, Zr and Nb, and a decrease in Cr and Ni for decreasing MgO (not all shown in Fig. 6). These trends are tholeiitic and can be attributed to the fractionation of olivine plus spinel, clino and orthopyroxene, and plagioclase, observed as micro-phenocrysts in the less fractionated lavas, as well as Fe-Ti oxides (ilmenite and Ti-magnetite) in the more evolved. Based on Nb/Y and Zr/TiO_2 ratios (Fig. 5c), the samples are tholeiitic, transitional and alkalic basalts. In the tectonic discrimination diagrams of Wood (1980) and Meschede (1986), they plot consistently in the within-plate tholeiitic and alkalic basalt fields (Fig. 5a, b). These patterns and the values of the Ti/V>20 (Fig. 5d) and Zr/Nb<15 (Fig. 6f) ratios, are characteristic of modern day transitional and alkalic oceanic-island basalts (Pearce, 2008). However, the existing compositional diversity indicates a different mantle source for the magmas of each geochemical group of the DFm. In this sense, the low contents of Ti and low absolute abundances of REE (~10xN) of the group I suggest a source dominated by depleted mantle; the higher TiO_2 and REE contents at a given MgO concentration, as well as the absence of Zr-Hf negative anomalies, of the group II suggest a more enriched magma source than in the group I; and the highest TiO_2 and REE contents at a given MgO concentration of the group III suggest a more enriched mantle source than in group II.

Figures 7 and 9 show the compositional ranges of the three groups of basalts sampled in the DFm, as well as those of several CLIP units in Hispaniola, Beata Ridge, SW Puerto Rico and Blue Mountain inlier of Jamaica. These data help us to strengthen the regional correlations between magmatic events previously based on geochronological arguments. As shown, the group I tholeiitic basalts are geochemically similar to the basalts of the Dumisseau Fm in the Massif de la Hotte analysed by Sinton et al. (2000), the dolerites and gabbros sampled in the Beata Ridge (Révillon et al., 2000), the basalts drilled at the DSDP Leg 15 (except 151 site; Sinton et al., 2000), the basalts of the Siete Cabezas Fm (Escuder-Viruete et al., 2008, 2010, 2011a) and the basalts of the Bath Dunrobin Fm of Jamaica (Hastie et al., 2009). The geochemical characteristics of all these tholeiites are common in most of the mafic lavas of the CLIP and suggest a similar relatively depleted mantle source (e.g., Kerr et al., 2002). The group II transitional basalts of the DFm are compositionally similar to the basalts of the DFm in Haiti analysed by Loewen et al. (2013), the basalts of the Pelona-Pico Duarte Fm in the Cordillera Central (Escuder-Viruete et al., 2011a), and the basalts of the north facies of the Upper Cajul Fm in SW Puerto Rico (Jolly et al., 2007; Lidiak et al., 2011) (Fig. 9). The group III alkaline basalts are comparable to basalts of the Beata Ridge (Révillon et al., 2000) and the south facies of the Upper Cajul Fm (Jolly et al., 2007). The geochemical characteristics of the groups II and III samples are typical of transitional and alkaline OIB and require a deeper and enriched garnet-bearing mantle source, than those for group I. In summary, petrological, geochemical and geochronological data indicate that the igneous basement of the Sierra de Bahoruco is compositionally similar and coeval with the extensive mafic volcanism of the late Cretaceous Caribbean plateau and, therefore, the DFm is an onland section the CLIP, which continues through the Beata Ridge.

Although, the volcanic rocks of the DFm exhibit a broad compositional diversity likely due to different melting histories, none of the three groups show evidence of a subduction component in their petrogenesis. i.e., they have no negative HFSE anomalies. Proxies of mantle-crust interaction

(Th-Nb) and melting depth (TiO_2-Nb) of Pearce (2008) indicate no involvement of the crust in generation of the DFm basalts (Fig. 10a; or Nb/Th>8 in Fig. 6e), either by direct crustal contamination or crustal recycling by subduction or via inherited subduction components in the lithosphere. Therefore, the tectonic block of the Sierra de Bahoruco shows no genetic relationship to the Caribbean island-arc, which forms the igneous basement in the northern and eastern sectors of the Dominican Republic.

6.4. Trace element modelling: dynamic melting and nature of the source

The petrogenesis of the DFm can be characterised through the trace element modelling of the mantle melting processes. The REE composition of a melt can be particularly diagnostic of the source mineralogy and degree of melting. For this reason, spinel lherzolite and garnet lherzolite melting models were used to test the influence of source mineralogy on REE concentrations, and on LREE/HREE and MREE/HREE ratios (in this study chrondrite-normalised $[La/Yb]_C$ and $[Tb/Yb]_C$). The results were the compared with the least evolved compositions of the DFm basalts.

The details of the model starting mineralogies, bulk partition coefficients, and source compositions are summarised in Escuder-Viruete et al. (2011a) and in Appendix D. The equation used to derive the melting curves in Fig. 11 is the aggregated non-modal fractional melting equation of Shaw (1970):

$$[x_i] = [x_o]\ (1/D_o)\ (1- ((P\ F)/D_o))^{(1/P-1)}$$

where x_i is the concentration in the liquid, x_o is the concentration in the source, D_o is the bulk partition coefficient, F is the degree of melting and P is the proportion each phase contributes to the melt. The results of these calculations suggest that the DFm basaltic melts may have been produced by variable amounts of melting in the garnet (~3.5-2.5 GPa) and spinel lherzolite (~2.5-0.9 GPa) stability fields (Fig. 11). The three geochemical groups defined in the DFm are characterised by different $[La/Yb]_C$ and $[Tb/Yb]_C$ ratios, which represent various modelled mixtures of melts produced in the garnet and spinel lherzolite fields and degrees of melting: group I tholeiites are shallow melts produced in the spinel lherzolite field; group II transitional basalts result from mixing of 25-40% melts produced at high P in the garnet lherzolite field with 60-75% melts produced at low pressure in the spinel lherzolite field; and group III alkaline basalts are formed from mixing of 75-85% melts produced in the garnet lherzolite field with 15-25% melts produced in the spinel lherzolite field. The results of the modelling also indicate that groups II and III samples represent aggregate melts formed by low melting extents (1-6%) at high-P, but group I samples require more extensive melting (4-15%) at low-P (Fig. 11). Therefore, tholeiitic, transitional and alkaline basalts can be interpreted as aggregate melts produced from melting throughout the depth of the melting column. Basaltic melts generated and incorporated at different mantle depths are most probably consequence of the melting processes in an upwelling heterogeneous plume (e.g., Kerr and Mahoney, 2007; Greene et al., 2009). On the other hand, field data often indicates that groups II and III magmas are older than group I magmas. If these relations are confirmed by new geochronological data, the sources of the DFm can be interpreted to have become shallower and more depleted over time, which is also consistent with the upwelling of a hot plume under the oceanic crust.

To further test this hypothesis, dynamic melting models were used to simulate the progressive decompression melting in a mantle plume. For the DFm basalts, the evolution of the trace element concentrations was simulated using the melting model of Zou and Reid (2001), in which mantle melting at P>1GPa involves incongruent melting with olivine being produced during the reaction: spinel+orthopyroxene+clinopyroxene = olivine+melt for spinel lherzolites. The model parameters and results are described in Fig. 12 and in the Appendix D. The modelling comprises three stages: (a) melting of garnet lherzolite to form group III alkaline basalts; (b) melting of garnet and spinel lherzolite to produce group II transitional basalts; and (c) melting of spinel lherzolite to formgroup I tholeiites. Alkaline basalts are consistent with a low degree of melting (0.05-4%) of garnet lherzolite

(Fig. 12a). Transitional basalts involved melting of both garnet and spinel lherzolite and represent aggregate melts produced from continuous melting throughout the melting column (Fig. 12b). The 2:3 to 1:3 ratios of garnet and spinel lherzolite melt provide the best results. Therefore, melts would have involved lesser amounts of deeper and enriched small-degree melts (1-6% melting) and greater proportions of shallower and depleted high-degree melts (3-9%). Tholeiites require high degrees of melting (8-20%) of a spinel lherzolite source (Fig. 12c), similar to results based on trace element ratios discussed above. On the other hand, the mantle potential temperatures for primary magma compositions computed using PRIMELT3 code (Herzberg and Asimow, 2015) are 1453-1517 ºC for tholeiites, 1473-1514 ºC for transitional basalts, and 1453-1492 ºC for alkaline rocks. These mantle temperatures are hotter than below oceanic spreading centres and are indicative of a thermal anomaly of 200-300ºC, which are consistent with a mantle plume source for the DFm rocks.

The Fig. 11 also includes the compositional fields of the CLIP units outcropping in Hispaniola (Escuder-Viruete et al., 2010, 2011a) and the Beata Ridge (Révillon et al., 2000), as well as the drilled basalts in the DSDP 146-153 sites (except 151; re-analysed by Jolly et al., 2007) in the Caribbean basin. As can be seen, the basalts of the Siete Cabezas Fm, the gabbros and dolerites of the Beata Ridge, and most of the samples from DSDP, are similar in composition to the melts modelled by melting of spinel lherzolite. The results indicate varying degrees of melting (from 1.5 to 15%) of this source, which are generally higher for the Siete Cabezas Fm. However, a small contribution of melts generated in the garnet stability field (<1%) cannot be ruled out. This shallow and relatively depleted source is similar to those of the group I tholeiites of the DFm. However, the basalts of the Pelona-Pico Duarte Fm, the Beata Ridge, and the DSDP 151 site are akin to melt mixtures involving a garnet lherzolite. This deep and relatively enriched source is similar to those of the groups II and III of the Dumisseau Fm, particularly the transitional basalts. The results of the dynamic melting models shown in the Fig. 12 also indicate the existence of different sources and melting histories in the petrogenesis of the DFm, as well as other units of the CLIP in the late Cretaceous. Transitional and alkaline basalts of the Dumisseau Fm in Haiti (Loewen et al., 2013), the Beata Ridge (Révillon et al., 2000) and the Upper Cajul Fm in SW Puerto Rico (Lolly et al., 2007; Lidiak et al., 2011), also involve deep melting of garnet and spinel lherzolites, while the dolerites and gabbros of the Beata Ridge require a higher degree of melting of a shallower and depleted spinel lherzolite. These relationships also reinforce that the DFm is part of the CLIP.

6.5. Tectonomagmatic model for the late Cretaceous magmatism of the CLIP

Fitton et al. (1997) and Kerr et al. (1997, 2002) have shown that CLIP basalts fall in the log Zr/Y-log Nb/Y diagram between the two lines that define the Iceland plume-derived lavas. In the Fig. 10b, the volcanic rocks of the DFm fall between these two lines, above the ΔNb line between plume and non-plume sources, which suggests that the parental magmas were also derived from a general plume-influenced source. In this sense, the range of Zr/Y values for the group I samples matches those of the MORB field (exemplified with the Eastern Pacific Rise MORB field), but at higher Nb/Y values and above the ΔNb line. The group I samples may derive therefore from melting of a Nb-enriched, shallow lherzolite source. This source could be located bellow, or near, a center of oceanic opening, or in areas of the Caribbean basin subject to contemporaneous lithospheric extension (Driscoll and Diebold, 1999; Révillon et al., 2000; Mauffret et al., 2000; Escuder-Viruete et al., 2008, 2011a). The geochemical similarity of basalts of the Siete Cabezas Fm, the dolerites and gabbros of the Beata Ridge, the DSDP Leg 15 and part of the Upper Cajul Fm of SW Puerto Rico suggests a similar shallow lherzolite source. The group III samples of the DFm and the South Facies of the Upper Cajul Fm plot at highest Zr/Y values, near the more enriched mantle sources, and may result from melting of a deeper and enriched source as garnet lherzolite. Group II samples also plot at high Zr/Y values in an intermediate position between groups I and III samples, and may derive from a mixture of respective spinel and garnet lherzolite sources, as basalts of the Pelona-Pico Duarte Fm, the DSDP

151 site, and the Dumisseau Fm in Haiti.

These petrogenetic relations can be explained by the model proposed by Escuder-Viruete et al. (2011a, 2013), in which the Campanian plume-related magmatism of the CLIP took place in the back-arc area of the intraoceanic Caribbean island arc. In the late Cretaceous, the SW-directed subduction of proto-Caribbean oceanic lithosphere produced the Caribbean arc migration toward the NE by rollback (Fig. 13). The initial extension of the island-arc induced by rollback (90-88 Ma), was later expanded to the back-arc area (85-80 Ma). Therefore, the upper Caribbean Plate would be subject to crustal extension processes, which eventually led to the opening of an oceanic ridge characterised by magmatism unaffected by subduction, particularly its SW side opposite to the arc. The ridge and/or the crustal extension produces melts whose shallow source would be modified by an enriched plume component, incorporated by lateral flow in the mantle from the SW. These relatively enriched MORB type melts would lead to the group I tholeiites of the DFm, as well as similar compositional basalts of other CLIP units of Campanian age. In contrast, the OIB type melts result from a deeper and enriched plume source, located in the back-arc area and unconnected with the centre of oceanic opening. These melts would result the transitional and alkaline basalts of the DFm and Pelona-Pico Duarte Fm during the 80-68 Ma time interval (Campanian-Maastrichtian). This tectonomagmatic model is compatible with the widespread and rapid eruption of basaltic flows associated with the extensional deformation of the Caribbean plate prior to the Campanian-Maastrichtian, based on the seismic data of Diebold et al. (1999) and Driscoll and Diebold (1999). The mantle plume process in the Caribbean basin may be similar to the Samoan and Louisville plumes affecting the opening of the Lau Basin (Wendt et al., 1997; Turner and Hawkesworth, 1998), or the plume-related back-arc spreading in the Norfolk Basin (Sdrolias et al., 2004). The arc-continent collision during the latest Maastrichtian to lower Eocene led to the cessation of the arc magmatism and, indirectly, to the volumetrically important episodes of plume magmatism in the

Caribbean back-arc basin.

ACKNOWLEDGEMENTS

The authors thank John Lewis, Gren Draper, Peter Baumgartner and many colleagues of the IGME and BRGM for help and discussions on the geology of the Dominican Republic. The Servicio Geológico Nacional of the Dominican Government is also thanked by support. David Buchs, Jörg Geldmacher, Andrew Kerr and Greg Shellnutt provided very careful and constructive reviews; their contributions have greatly improved the previous version of the manuscript. This work is part of the CGL2012-33669/BTE project, and also received aid from the mapping project of the Dominican Republic funded by the SYSMIN Program of the European Union.

REFERENCES

Abad, M. (2010). Mapa Geológico de la Hoja a E. 1:50.000 nº 5969-I (Enriquillo) y Memoria correspondiente. Proyecto 1B de Cartografía Geotemática de la República Dominicana. Programa SYSMIN. Dirección General de Minería, Santo Domingo. 202 pp.

Bandini, A.N., Baumgartner, P.O., Flores, K., Dumitrica, P., Jackett, S.J., 2011. Early Jurassic to early Late Cretaceous radiolarians from the Santa Rosa accretionary complex (northwestern Costa Rica), *Ofioliti*, 36(1), 1–35.

Baumgartner, P.O., Flores, K., Bandini, A.N., Girault, F. and Cruz, D., 2008. Late Triassic to Cretaceous Radiolaria from Nicaragua and Northern Costa Rica-The Mesquito Oceanic terrane. *Ofioliti*, 33, 1-19.

Bienvenu, P., Bougault H., Joron J.L., Treuil, M., Demitriev, L., 1990. REE/non REE element hygromagmaphile element fractionation. *Chemical Geology*, 82, 1–14

Buchs, D. M., Arculus, R.J., Baumgartner, P.O., Baumgartner-Mora, C., Ulianov, A., 2010. Late Cretaceous arc development on the SW margin of the Caribbean Plate: Insights from the

Golfito, Costa Rica, and Azuero, Panama, complexes, *Geochemistry, Geophysics, Geosystems*, 11(7), Q07S24.

Calmus, T., 1983. Contribution a l'etude geologique du Massif de Macaya (Sud-ouest d'Haiti, Grandes Antilles), sa place dans l'evolution de l'orogene Nord-Caraibe. These Docteur de 3er Cycle, L'Univ. Pierre et Marie Curie, Paris, 163 pp.

Condie, K.C., 2005. High field strength element ratios in Archean basalts: A window to evolving sources of mantle plumes?, Lithos, 79, 491-504.

De León, R.O. (1989). Geología de la Sierra de Bahoruco (República Dominicana). Museo Nacional de Historia Natural. Santo Domingo, 112 p.

Denyer, P., Baumgartner, P.O., Gazel, E., 2006. Characterization and tectonic implications of Mesozoic-Cenozoic oceanic assemblages of Costa Rica and Western Panama, *Geologica Acta*, 4(1–2), 219–235.

Diebold, J. B., N. W. Driscoll, and EW-9501 Science Team, 1999. New insights on the formation of the Caribbean Basalt Province revealed by multichannel seismic images of volcanic structures in the Venezuelan Basin. In Mann, P. (ed) Caribbean Basins, Sedimentary Basins World, Elsevier Sci., Amsterdam. 4, 561–589.

Donnelly, T.W., 1994. The Caribbean Cretaceous basalt association: A vast igneous province that includes the Nicoya complex of Costa Rica. In: Seyfried, H., Hellman, W. (eds.). Geology of an Evolving Island Arc: The Isthmus of Southern Nicaragua, Costa Rica, and Western Panama: Stuttgart, Germany, Profile (Band 7). Institut für Geologie und Palaontologie, 17-45.

Donnelly, T.W., Beets, D., Carr, M.J., Jackson, T., Klaver, G., Lewis, J., Maury, R., Schellenkens, H., Smith, A.L., Wadge, G., Westercamp, D., 1990. History and tectonic setting of Caribbean magmatism. In: Dengo, G., Case, J. (eds), The Caribbean Region. Vol. H. The Geology of North America. *Geological Society of America*, 339–374.

Driscoll, N. W., and J. B. Diebold (1999), Tectonic and stratigraphic development of the eastern

Caribbean: New constraints from multichannel seismic data. In Mann, P. (ed) Caribbean Basins, Sedimentary Basins World, Elsevier Sci., Amsterdam. 4, 591–626.

Duncan, R. A., Hargraves, R. B. 1984. Plate tectonic evolution of the Caribbean region in the mantle reference frame. In: Bonini, W. E., Hargraves, R. B. & Shagam, R. (eds) The Caribbean-South American plate boundary and regional tectonics. *Geological Society of America, Memoir*, 162, 81-93.

Escuder-Viruete, J., 2010. Mapa Geológico de la República Dominicana E. 1:50.000. Informe (Parte 1) de Petrología de Rocas Ígneas y Metamórficas, Hojas de Polo, La Ciénaga, Enriquillo, Sabana Buey y Nizao. Dirección General de Minería, Santo Domingo, 33 pp.

Escuder-Viruete, J., Pérez-Estaún, A., Contreras, F., Joubert, M., Weis, D., Ullrich, T.D., Spadea, P., 2007. Plume mantle source heterogeneity through time: insights from the Duarte Complex, Central Hispaniola. *Journal of Geophysical Research*, 112, B04203. doi: 10.1029/2006JB004323.

Escuder-Viruete, J., Joubert, M., Urien, P., Friedman, R., Weis, D., Ullrich, T., Pérez-Estaún, A., 2008. Caribbean island-arc rifting and back-arc basin development in the Late Cretaceous: geochemical, isotopic and geochronological evidence from Central Hispaniola. *Lithos*, 104, 378-404. doi:10.1016/j.lithos.2008.01.003.

Escuder-Viruete, J., Pérez-Estaún, A., Weis, D., 2010. Geochemical constraints on the origin of the late Jurassic proto-Caribbean oceanic crust in Hispaniola. *International Journal of Earth Sciences*, 98, 407-425. doi: 10.1007/s00531-007-0253-4.

Escuder-Viruete, J., Pérez-Estaún, A., Joubert, M., Weis, D. 2011a. The Pelona-Pico Duarte basalts Formation, Central Hispaniola. An on-land section of Late Cretaceous volcanism related to the Caribbean large-igneous province. *Geologica Acta*, 9(3–4), 1–22.

Escuder-Viruete, J., Pérez-Estaún, A., Booth-Rea, G., Valverde-Vaquero, P., 2011b. Tectono-metamorphic evolution of the Samaná complex, northern Hispaniola: implications for the burial and exhumation of high-pressure rocks in accretionary wedges. Lithos 125, 190-210.

Escuder-Viruete, J., Valverde-Vaquero, P., Rojas-Agramonte, Y., Gabites, J., Pérez-Estaún, A., (2013). From intra-oceanic subduction to arc accretion and arc-continent collision: Insights from the structural evolution of the Río San Juan metamorphic complex, northern Hispaniola. *Journal of Structural Geology*, 46, 34-56. doi: 10.1016/j.jsg.2012.10.008

Escuder-Viruete, J., Valverde-Vaquero, P., Rojas-Agramonte, Y., Castillo-Carrión, M., Gabites, J., Pérez-Estaún, A., 2013. Timing of deformative events in the Río San Juan complex, northern Hispaniola: implications for the tectonic controls on the exhumation of high-P rocks in the northern Caribbean subduction-accretionary wedge. Lithos 177, 416-435. http://dx.doi.org/10.1016/j.lithos.2013.07.006

Fitton, J.G., Saunders, A.D., Norry, M.J., Hardarson, B.S., Taylor, R.N., 1997. Thermal and chemical structure of the Iceland plume. *Earth Planetary Science Letters*, 153: 197– 208

Gradstein, F.M., Ogg, J.G., Schmitz, M.D., and Ogg, G.M., editors, 2012, The Geologic Time Scale 2012, vol. 1: Boston, Elsevier, 1144 p., http://dx.doi.org/10.1016/B978-0-444-59425-9.01001-5.

Greene, A.R., Scoates, J.S., Weis, D., Nixon, G.T., Kieffer, B., 2009. Melting history and magmatic evolution of basalts and picrites from the accreted Wrangellia oceanic plateau on Vancouver Island, Canada. Journal of Petrology 50, 467-505.

Hastie, A.R., A.C. Kerr, 2010. Mantle plume or slab window?: Physical and geochemical constraints on the origin of the Caribbean oceanic plateau, Earth Science Review 98(3–4), 283–293. doi:10.1016/j.earscirev.2009.11.001.

Hastie, A.R., Kerr, A.C., Mitchell, S.F., Millar, I.L., 2008. Geochemistry and petrogenesis of Cretaceous oceanic plateau lavas in eastern Jamaica. *Lithos*, 101, 323-343.

Hastie, A.R., Kerr, A.C., Mitchell, S.F., Millar, I.L., 2009. Geochemistry and tectonomagmatic significance of Lower Cretaceous island arc lavas from the Devils Racecourse Formation, eastern Jamaica. In: James, K.H., Lorente, M.A., Pindell, J.L. (eds) The Origin and Evolution of the Caribbean Plate. Geological Society, London, Special Publications, 328, 339–360.Hauff, F., Hoernle K.A., van den Bogaard, P., Alvarado G.E., Garbe-Schönberg, D. 2000. Age and geochemistry of basaltic complexes in western Costa Rica: Contributions to the geotectonic evolution of Central America, *Geochemistry*, *Geophysics*, *Geosystems*, 1(5), 1009, doi:10.1029/1999GC000020.

Herzberg, C, Asimow, P.D., 2015. PRIMELT3 MEGA.XLSM software for primary magma calculation: Peridotite primary magma MgO contents from the liquidus to the solidus, Geochemistry, Geophysics, Geosystems, 16, doi:10.1002/2014GC005631.

Hoernle, K., Hauff, F., Bogaard, P. van den, 2004. A 70 Myr history (139–69 Ma) for the Caribbean large-igneous province, Geology, 32, 697–700, doi:10.1130/G20574.1.

James, K.H., 2009, In situ origin of the Caribbean: Discussion of data. In: James, K.H., Lorente, M.A., and Pindell, J.L. (eds) The origin and evolution of the Caribbean Plate. Geological Society London Special Publication 328, 77–125.

Jolly, W.T., Schellekens, J.H., Dickin, A.P., 2007. High-Mg andesites and related lavas from southwestern Puerto Rico (Greater Antilles Island Arc): petrogenetic links with emplacement of the Caribbean mantle plume. *Lithos*, 98, 1–26.

Joubert, M., 2010. Mapa Geológico de la Hoja a E. 1:50.000 nº 5970-II (La Ciénaga) y Memoria correspondiente. Proyecto 1B de Cartografía Geotemática de la República Dominicana. Programa SYSMIN. Dirección General de Minería, Santo Domingo. 202 pp.

Kerr, A.C., 2003. Oceanic plateaus. In: Rudnick, R. (ed.), The Crust. Treatise on Geochemistry, vol. 3. Elsevier Science, pp. 537–565.

Kerr, A.C., Tarney. J., 2005. Tectonic evolution of the Caribbean and northwestern South America: The case for accretion of two Late Cretaceous oceanic plateaus. *Geology*, 33, 269–272

Kerr, A.C., Tarney, J., Marriner, G.F., Nivia, A., Saunders, A.D., 1997. The Caribbean–Colombian

Cretaceous igneous province: The internal anatomy of an oceanic plateau. In: Mahoney, J., Coffin, M.F. (Eds), Large-igneous Provinces. AGU Washington DC. pp. 123–144.

Kerr, A.C., Tarney, J., Kempton, P.D., Spadea, P., Nivia, A., Marriner, G.F., Duncan, R.A., 2002. Pervasive mantle plume head heterogeneity: evidence from the late Cretaceous Caribbean–Colombian oceanic plateau. *Journal of Geophysical Research*, 107 (B7), 10.1029/ 2001JB000790

Kerr, A.C., White, R.V., Thompson, P.M.E., Tarney, J., Saunders, A.D., 2003. No oceanic plateau-No Caribbean Plate? The seminal role of an oceanic plateau in Caribbean Plate evolution. In: Bartolini, C., Buffler, R.T., and Blickwede, J.F. (eds.) The circum-Gulf of Mexico and Caribbean region; Hydrocarbon habitats, basin formation, and plate tectonics. Tulsa, American Association of Petroleum Geologists Memoir 79, 126–168.

Kerr, A. C., D. G. Pearson, and G. M. Nowell (2009), Magma source evolution beneath the Caribbean oceanic plateau: New insights from elemental and Sr-Nd-Pb-Hf isotopic studies of ODP Leg 165 Site 1001 basalts, Geol. Soc. Spec. Publ., 328(1), 809–827, doi:10.1144/SP328.31.

Lapierre, H., Dupui, V., Lepinay, B.M., Tardy, M., Ruiz, J., Maury, R.C., Hernandez, J., Loubert, M., 1997. Is the Lower Duarte Complex (Hispañiola) a remnant of the Caribbean plume generated oceanic plateau? *Journal of Geology*, 105, 111–120.

Lapierre, H., Bosch, D., Dupuis, V., Polvé, M., Maury, R., Hernandez, J., Monié, P., Yeghicheyan, D., Jaillard, E., Tardy, M., de Lepinay, B., Mamberti, M., Desmet, A., Keller F., Senebier, F., 2000. Multiple plume events in the genesis of the peri-Caribbean Cretaceous oceanic plateau province. *Journal of Geophysical Research*, 105, 8403-8421.

Lewis, J.F., Draper, G., 1990. Geological and tectonic evolution of the northern Caribbean margin. In: The Geology of North America (Dengo, G., Case, J.E., Eds.), Vol. H, The Caribbean region. *Geological Society of America*, 77-140.

Lewis, J.F., Escuder-Viruete, J., Hernaiz Huerta, P.P., Gutiérrez, G., Draper, G., 2002. Subdivisión Geoquímica del Arco Isla Circum-Caribeño, Cordillera Central Dominicana: Implicaciones para la formación, acreción y crecimiento cortical en un ambiente intraoceánico. *Acta Geológica Hispánica*, 37, 81-122.

Lidiak, E.G., Jolly W.T., Dickin A.P., 2011. Pre-arc basement complex and overlying early island arc strata, Southwestern Puerto Rico: overview, geologic evolution, and revised data bases. Geologica Acta, 9 (3-4) 273-287.

Llinás, R.A., 1972. Geología del área Polo-Duvergé, Cuenca de Enriquillo, República Dominicana. Tesis Doctoral. Universidad Nacional Autónoma de México, Facultad de Ingeniería, 83 p.

Loewen, M.W., Duncan, R.A., Kent, A.J.R., Krawl, K., 2013. Prolonged plume volcanism in the Caribbean Large Igneous Province: New insights from Curaçao and Haiti, Geochem. Geophys. Geosyst., 14, 4241–4259, doi:10.1002/ggge.20273.

McPhie, J., Doyle, M, Allen, R., 1993. Volcanic textures: a guide to the interpretation of textures in volcanic rocks. Centre for Ore Deposit and Exploration Studies, University of Tasmania, 198 pages.

Mann P., Draper G., Lewis, J.F., 1991. An overview of the geologic and tectonic development of Hispaniola. In: Geologic and tectonic development of the North America-Caribbean plate boundary in Hispaniola (Mann P., Draper G., Lewis J.F. Eds.). *Geological Society of America Special Paper*, 262, 1-28.

Mann, P., Calais, E., Ruegg, J.C., Demets C., Jansma, P.E. and Mattioli, G.S. 2002. Oblique collision in the northeastern Caribbean from GPS measurements and geological observations. Tectonics 21, 6, 1- 26.

Mann, P., Rogers, R., Gahagan, L., 2007. Overview of plate tectonic history and its unresolved tectonic problems. Bundschuh, J., and Alvarado, G.E. (eds) Central America: Geology, Resources and Hazards, v. 1. Leiden. The Netherlands, Taylor and Francis/Balkema, 201-

237.

Mauffret, A., Leroy, S. 1997. Seismic stratigraphy and structure of the Caribbean igneous province. *Tectonophysics*, 283, l61–104.

Mauffret, A., Leroy, S., Vila, J.M., Hallot, E., Mercier de Lépinay, B., Duncan, R.A., 2000. Prolonged magmatic and tectonic development of the Caribbean Igneous Province revealed by a diving submersible survey. Marine Geophysical Researches, 22, 17-45.

Maurrasse, F.J.M., G., Husler, J., Georges, G., Schmitt, R., Damond, P., 1979. Upraised Caribbean sea-floor below acoustic reflector B" and the Southern Peninsula of Haiti. *Geologie en Mijnbuow*, 8, 71-83.

Montes, C., G. Bayona, A. Cardona, D. M. Buchs, C. A. Silva, S. Morón, N. Hoyos, D. A. Ramírez, C. A. Jaramillo, and V. Valencia (2012), Arc-continent collision and orocline formation: Closing of the Central American seaway, J. Geophys. Res., 117, B04105, doi:10.1029/2011JB008959.

Montgomery, H., Pessagno, E.A., Lewis, J.F., Schellekens, J., 1994. Paleogeography of Jurassic fragments in the Caribbean. *Tectonics*, 13, 725-732.

Montgomery, H., Pessagno, E.A., 1999. Cretaceous microfaunas of the Blue mountains, Jamaica, and of the Northern and Central Basement Complexes of Hispaniola. Caribbean. In Mann, P., (ed) Caribbean Basins. Sedimentary Basins of the Word, v. 4, p. 237-246.

Montgomery, H., Kerr, A.C., 2009. Rethinking the origins of the red chert at La Désirade, French West Indies. In. James, K., Lorente, M. A. & Pindell, J. (eds) The geology and evolution of the region between North and South America, Geological Society of London, Special Publication. 328, 457–467.

Pearce, J.A., 2008. Geochemical fingerprinting of oceanic basalts with applications to ophiolite classification and the search for Archean oceanic crust. Lithos 100, 14–48.

Pérez-Valera, F., 2010. Mapa Geológico de la Hoja a E. 1:50.000 nº 5970-III (Polo) y Memoria correspondiente. Proyecto 1B de Cartografía Geotemática de la República Dominicana. Programa SYSMIN. Dirección General de Minería, Santo Domingo.

Pérez-Valera, F., Abad, M., 2010. Informe Estratigráfico y Sedimentológico. Proyecto de Cartografía Geotemática de la República Dominicana. Programa SYSMIN, Proyecto 1B. Consorcio IGME-BRGM-INYPSA. Dirección General de Minería, Santo Domingo, 168 pp.

Pindell, J., Kennan, L., Maresch, W.V., Stanek, K.P., Draper, G., Higgs, R. 2005. Plate-kinematics and crustal dynamics of circum-Caribbean arc-continent interactions: Tectonic controls on basin development in Proto-Caribbean margins. In: Lallemant, A. and Sisson V.B. (e,ds.), Caribbean-South American plate interactions. *Geological Society of America Special Paper*, 394, 7-52.

Pindell, J., Kennan, L., 2009. Tectonic evolution of the Gulf of Mexico, Caribbean and northern South America in the mantle reference frame: an update. In. James, K., Lorente, M. A. & Pindell, J. (eds) The geology and evolution of the region between North and South America, *Geological Society of London, Special Publication*. 328, 1-55.

Révillon, S., Hallot, E., Arndt, N., Chauvel, C., Duncan, R.A., 2000. A Complex History for the Caribbean Plateau: Petrology, Geochemistry, and Geochronology of the Beata Ridge, South Hispaniola. *Journal of Geology*, 108, 641–661.

Salters, V.J.M., Stracke, A., 2004. Composition of the depleted mantle, Geochemistry, Geophysics, Geosystems, 5, doi: 10.1029/2003GC000597.

Sandoval, M.I., Baumgartner, P.O., Escuder-Viruete, J., Gabites, J., Mercier de Lépinay, B., 2015. Late Cretaceous radiolarian biochronology of the Pedro Brand section, Tireo Group, eastern Central Cordillera, Dominican Republic: a contribution to the Caribbean Large Igneous Province stratigraphy. *Revue de Micropaléontologie*. 58, 85-106.

Sdrolias, M., Dietmar Müller, R., Mauffret, A., Bernardel, G., 2004. Enigmatic formation of the Norfolk Basin, SW Pacific: A plume influence on back-arc extension. Geochemistry, Geophysics, Geosystems, 5 (6), Q06005. doi:10.1029/2003GC000643

Sen, G., Hickey-Vargas, D.G., Waggoner, F., and Maurrasse, F., 1988, Geochemistry of basalts from the Dumisseau Formation. Southern Haiti: Implications for the origin of the Caribbean Sea crust. *Earth Planetary Science Letters,* 87, 423-437.

Shaw, D.M., 1970. Trace element fractionation during anatexis. Geochimica et Cosmochimica Acta, 34, 237-243.

Sinton, C.W., Duncan, R.A., Storey, M., Lewis, J., Estrada, J.J., 1998. An oceanic flood basalt province within the Caribbean plate. *Earth Planetary Science Letters*, 155, 221– 235.

Sinton, C. W., H. Sigurdsson, and R. A. Duncan (2000), Geochronology and petrology of the igneous basement at the lower Nicaraguan Rise. *Proceedings of the Ocean Drilling Program, Scientific Results*. 165, 233–236.

Sun, S.S., McDonough, W.F., 1989. Chemical and isotopic systematics of oceanic basalts: Implications for mantle compositions and processes. In: Saunders, A.D., Norry, M.J. (Eds), Magmatism in the Ocean Basins. *Geological Society of London Special Publication*, 42, 313-345.

Thompson, P.M.E., Kempton, P.D., White, R.V., Saunders, A.D., Kerr, A.C., Tarney, J., Pringle, M.S., 2004. Elemental, Hf-Nd isotopic and geochronological constraints on an island arc sequence associated with the Cretaceous Caribbean Plateau: Bonaire, Dutch Antilles. *Lithos*, 74, 91-116.

Turner, S., Hawkesworth, C., 1998. Using geochemistry to map mantle flow beneath the Lau Basin, Geology, 26, 1019–1022.

van Den Berghe, B., 1983. Evolution sedimetaire et structurale depuis le Paleocene de secteur Massif de la Selle-Barouco-Nord de la Ride de Beata dans l'orogene nor Caraibe (Hispaniola Grandes Antilles). These de doctorat, Universidad Marie y Pierre Curie, Paris, 205 pp.

Wendt, J. I., Regelous, M., Collerson, K.D., Ewart, A., 1997. Evidence for a contribution from two mantle plumes to Island Arc lavas from Northern Tonga, Geology, 25, 611-614.

Wood, D.A., 1980. The application of a Th-Hf-Ta diagram to problems of tectonomagmatic classification and to establishing the nature of crustal contamination of basaltic lavas of the British Tertiary volcanic province. *Earth Planetary Science Letters*, 50, 11-30.

Whattam, S.A., Stern, R.J., 2015. Late Cretaceous plume-induced subduction initiation along the southern margin of the Caribbean and NW South America: The first documented example with implications for the onset of plate tectonics. *Gondwana Research* 27, 38–63

Wright, J.E., Wyld, S.J., 2011. Late Cretaceous subduction initiation on the eastern margin of the Caribbean-Colombian Oceanic Plateau: One great arc of the Caribbean (?), Geosphere, 7(2), 468–493, doi:10.1130/GES00577.S3.

Zou, H., Reid, M.R., 2001. Quantitative modeling of trace element fractionation during incongruent dynamic melting. Geochimica et Cosmochimica Acta 65, 153–162.

FIGURE CAPTIONS

Fig. 1. (a) Map of the northeastern Caribbean plate margin (see inset for location in the Caribbean) showing location of the on land CLIP units (in red), plate boundaries and main tectonic features. The position of the DSDP sites (Legs 4 and 13), ODP Sites (Leg 165) and *Nautica* dive locations (triangles; Révillon et al., 2000) are indicated. SFZ, Septentrional fault zone; EPGFZ; Enriquillo-Platain Garden Fault Zone, CGFZ; Cerro Golden Fault Zone; MTB, Muertos Thrust Belt; MP, Mona Passage; MC, Mona Canyon; NHDB, North Hispaniola Deformed Belt; HP, Haiti Plateau; BE, Beata Escarpement; HE, Hess Escarpement; VDB, Venezuela Deformed Belt. CLIP units in the Cordillera Central: DC; Duarte Complex, SC; Siete Cabezas Fm; PPD; Pelona-Pico Duarte Fm. Other CLIP units: DF; Dumisseau Fm, BD; Bath-Dunrobin Fm, SWPR; SW Puerto Rico. (b) Simplified geological map of southern Hispaniola including the Sierra de Bahoruco in the Dominican Republic. Box shows location

of the studied area. (c) Schematic geological map of the eastern Sierra de Bahoruco (mod. from Abad, 2010; Joubert, 2010; Pérez Valera, 2010) showing location of samples collected in the Dumisseau Formation.

Fig. 2. Microphotographs of the volcanic rocks: (a) Olivine (Ol) micro-phyric basalt, PPL. (b) Elongated orthopyroxene (Opx) and clinopyroxene (Cpx) phyric basalt. Note twining in the titano-augite fenocryst. (c) Ortho and clinopyroxene phyric basalt. (d) Clinopyroxene and plagioclase (Pl) afanitic basalt, PPL. (e) Vesicular and altered andesitic basalt, PPL. (f) Polygenetic, lithic and basaltic breccia and microbreccia; (g) coarse-grained vitric tuff; and (h) Ortho and clinopyroxene bearing dolerite, PPL. Width of field=5 mm, except in (a) where width of field=2.2 mm. PPL=plane polarised light.

Fig. 3. Microphotographs of the altered volcanic rocks: (a) Microgabbro con hydrothermal alteration. Note elongated plagioclase (Pl) variably pseudomorphed by albite (Ab) and Fe-rich epidote (Ep) in a re-crystallised matrix of albite, epidote, chlorite (Chl) and sericite (Ser). PPL. (b) Plagioclase-phyric basalt afected by the hydrothermal alteration. Note the neoformation of brown mica (Bt), white mica (Ms), chlorite and albite, PPL. Width of field=5 mm. PPL=plane polarised light.

Fig. 4. (a and b) $^{40}Ar/^{39}Ar$ spectrum of whole rock in samples from Dumisseau Fm in the Sierra de Bahoruco. The plateau ages were calculated following techniques described in Appendix A. Plateau steps are filled and rejected open. (c) Schematic stratigraphic columns of the CLIP in several areas of the northeastern Caribbean Plate, including a summary of palaeontological and geochronological ages. Sources: (a) Kerr et al. (1997, 2002, 2009); (b) Sen et al. (1988); (c) Révillon et al. (2000); (d) Jolly et al. (2007); (e) Escuder-Viruete et al. (2007, 2009; 2011); (f) Sinton et al. (1998); (g) Hastie et al. (2009); (h) Loewen et al. (2013); and (i) this work. MMqCh, Middle Mariquita Chert; UMqCh, Upper Mariquita Chert; UCj, Upper Cajul Fm; Bqn, Boquerón Fm; SbG, Sabana Grande Fm; CFm, Constanza Fm; RFm, Restauración

Fm; PB, Peña Blanca Fm; PPD, Pelona-Pico Duarte basalts Fm; SC, Siete Cabezas Fm. 40Ar-39Ar ages include the error bars (in 2σ). Yellow bands correspond to the age ranges obtained for the three main building phases of the CLIP. Time scale from Gradstein et al., (2012).

Fig. 5. (a) Hf-Nb-Th diagram with fields defined by Wood (1980), (b) Nb-Zr-Y plot with fields defined by Meschede (1986), (c) Nb/Y versus Zr/TiO_2 diagram of Winchester and Floyd (1977), and (d) Ti-V diagram for volcanic rocks of the Dumisseau Fm in Sierra de Bahoruco.

Fig. 6. TiO_2, Al_2O_3, Fe_2O_3, Nb, Zr/Nb versus MgO, and Nb/Th versus Y, for the volcanic rocks of the Dumisseau Fm in Sierra de Bahoruco. Data from the Beata Ridge (Révillon et al., 2000), DSDP drilling sites (Sinton et al., 1998; Jolly et al., 2007; Lidiak et al., 2011), Pelona-Pico Duarte and Siete Cabezas Fm (Escuder-Viruete et al., 2009, 2010, 2011), northern (N) and southern (S) facies of the Upper Cajul Fm in SW Puerto Rico (Jolly et al., 2007; Lidiak et al., 2011) and the Dumisseau Fm in Haiti (Sen et al., 1988; Loewen et al., 2013) are shown for comparisons. Also indicated in (a) are 5% fractional crystallization vectors for olivine (Ol), clinopyroxene (Cpx), and plagioclase (Pl), determined from an average composition.

Fig. 7. N-MORB-normalised multi-element plots for the volcanic rocks of the Dumisseau Fm in the Sierra de Bahoruco: (a) group I, (b) group II, (c) group III, and (d) samples of Dumisseau Fm from the Massif de la Hotte in Haiti (for references see Fig. 6). Normalisation values are taken from Sun and McDonough (1989).

Fig. 8. Primitive mantle-normalised extended REE plots for the volcanic rocks of the Dumisseau Fm in the Sierra de Bahoruco and Haiti, Beata Ridge, DSDP Leg 15, and Cajul Fm of SW Puerto Rico. Normalisation values are taken from Sun and McDonough (1989).

Fig. 9. N-MORB-normalised multi-element plots for the geochemically groups defined in the Dumisseau Fm, which are compared to representative CLIP units of the northeastern Caribbean Plate (for references of the data see Fig. 6).

Fig. 10. Samples of the Dumisseau Fm in the Sierra de Bahoruco plotted in the Nb/Yb vs Th/Yb (Pearce, 2008) and Nb/Y vs Zr/Y (Fitton et al., 1997) log-log diagrams. Fields of fragments of the CLIP in SW Puerto Rico, Jamaica, and Beata Ridge, as well as the Dumisseau Fm in Haiti, the Pelona-Pico Duarte and the Siete Cabezas Fm in the Dominican Republic are also plotted (references in Fig. 6). In (a) MORB-OIB array, average composition of continental crust (CC) and Archean crust (A), % of subduction zone (SZ) component in the wedge and assimilation-fractional crystallization (AFC) models are from Pearce (2008), and the Caribbean island arc data in Hispaniola compiled by Escuder-Viruete et al. (2009, 2010). All geochemical groups of the DFm in the Sierra of Bahoruco lie within the MORB-OIB array, as well as data of the other late Cretaceous CLIP units, suggesting mantle sources variably modified by an enriched mantle component, without interaction with a crustal input by contamination or subduction. In (b) the different geochemical groups of the DFm and CLIP units plot within the tramlines defined by Icelandic mantle plume lavas. Abbreviations: PM; primitive mantle, DM; shallow depleted mantle, EM1 and EM2; enriched mantle sources; MORB; normal ocean ridge basalt, OIB; oceanic island basalt (from Condie, 2005).

Fig. 11. (a) and (b) $(La/Yb)_C$ versus $(Tb/Yb)_C$ diagrams with the results of the non-modal aggregated melt calculations for spinel lherzolite and garnet lherzolite assemblages (solid lines). Grey lines shows mixing between melts produced by variably degrees of spinel lherzolite melt mixed with 1.2% to 4.0% melt of garnet lherzolite. Open star in the lower left hand corner is the depleted mantle composition of Salters and Stracke (2004), used as the source in the modelling (for details see Appendix D). The arrow on the right in (b) shows the general direction in which crystal fractionation proceeds. Both group II and III basalts of the Dumisseau Fm plot well above the curve generated for spinel lherzolite melting in the diagram, suggesting that part of the melt generation for these types occurred in the garnet lherzolite field. A similar source can be established for the Pelona-Pico Duarte Fm and Beata

Ridge basalts, as well as samples of 151-site of the DSDP (references in Fig. 6). In contrast, group I basalts and samples of the Siete Cabezas Fm, as well as samples from the DSDP sites and gabbros and dolerites of the Beata Ridge, plot on the lower left side of the diagrams (see detail in b), indicating that melts produced by melting in the spinel lherzolite field (i.e. at lower pressure).

Fig. 12. Trace-element modelling results for incongruent dynamic mantle melting for basalts of the Dumisseau Fm following the melting model of Zou and Reid (2001). Three stages were considered in the modelling: (a) melting of garnet lherzolite compared with group III alkaline basalts; (b) melting of garnet and spinel lherzolite compared with group II transitional basalts; and (c) melting of spinel lherzolite compared with group I tholeiites. The results are indicated with grey curves and labels, which mean % of melting of each source. A 2:3 ratio of garnet and spinel lherzolite melt is indicate in (b), which means that for example 5% melting, 1% melt in garnet facies and 4% melt in spinel facies. A combination of 0.8PM+0.1DM components (PM, primitive mantle of Sun and McDonough, 1998; DM, depleted MORB mantle of Salters and Stracke, 2004) was selected as source composition. Details of the used source composition, mineralogy, melt reaction coefficients and partition coefficients of spinel and garnet lherzolites are included in the Appendix D.

Fig. 13. Tectonomagmatic model for the evolution of the northern margin of the Caribbean Plate, modified from Escuder-Viruete et al. (2011a, 2013). (a) After accretion/underplating of terranes beneath the intra-oceanic Caribbean island-arc, trench roll-back is accompanied by (composite) Caribbean arc extension, magmatic front migration and resumption of arc magmatism. Avanced arc rifting induces sinistral transpression and transtension, as well as syn-tectonic tonalitic plutonism in the Central Cordillera. Forearc and trench turbiditic sequences are deposited over and in front the subduction-accretionary complex. Plume-related magmatism in the CLIP is located in the Caribbean back-arc region. DC; Duarte

Complex, CF; Constanza Fm. (b) After Caribbean island-arc-North America continent collision (~60±5 Ma) the subsequent tectonic evolution is controlled by the suture-zone formation, the accretion of continental margin units (structural nappes) to the accretionary wedge and their sequential exhumation by thrusting, following a northeastward propagation of deformation. (c) As a result of migration from the trench, in the Caribbean back-arc and intra-arc regions basins are formed (in the last case of unknown amplitude). Much of the Caribbean plate was probably subjected to extension during this stage (Driscoll and Diebold, 1999) and, favouring the formation of MORB-like magmas by melting of a shallow enriched source. Melts derived from a deeper Caribbean-plume enriched source are incorporated by lateral flow from the SW and produced the OIB-like magmatism of the DFm. (d) Paleogene evolution is characterised by the transfer of the collisional deformation to the intra- and back-arc regions, where back thrusting and subduction polarity reversal took place (Kroehler et al., 2011). As result, SW-directed compressional structures are formed with uplift of the Central Cordillera. Subduction at the Los Muertos trench leads to the approach of the part of the CLIP, which is composed by the Beata Ridge and the Sierra de Bahoruco-Chaîne de la Serre. (e) The Neogene and Quaternary evolution is characterised by the docking of the Sierra de Bahoruco block, which cause its compressional deformation and uplift.

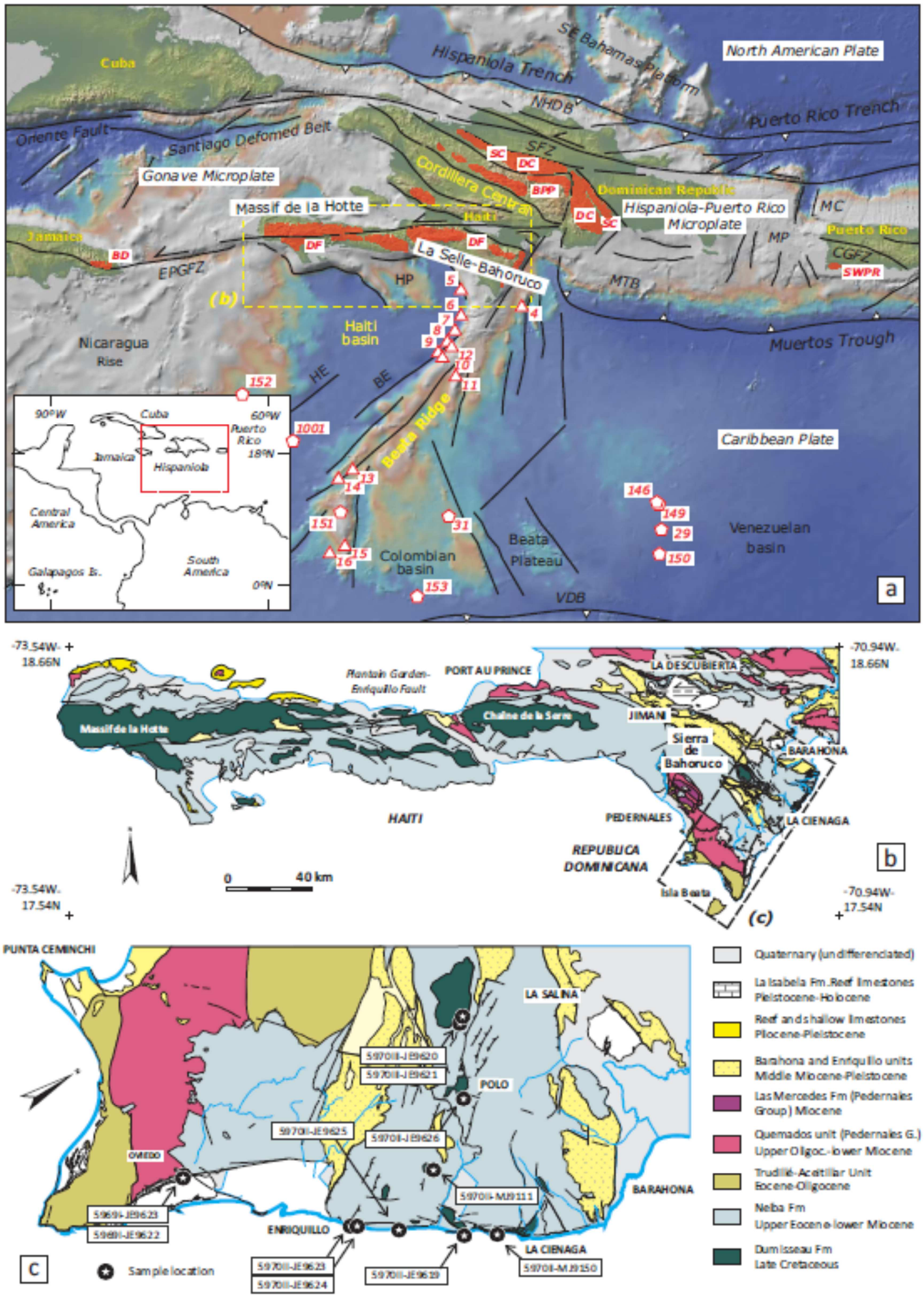
Cuba
Hispaniola Trench
SE Bahamas Platform
North American Plate
NHDB
Puerto Rico Trench
Oriente Fault
Santiago Defomed Belt
SFZ
Gonave Microplate
Cordillera Central
SC
DC
BPP
Dominican Republic
Massif de la Hotte
Haiti
DC
SC
Hispaniola-Puerto Rico Microplate
MC
MP
Puerto Rico
Jamaica
BD
DF
DF
La Selle-Bahoruco
CGFZ
SWPR
EPGFZ
HP
MTB
(b)
Nicaragua Rise
Halti basin
Muertos Trough
HE
BE
Beata Ridge
152
1001
Caribbean Plate
146
149
29
150
151
31
153
Colombian basin
Beata Plateau
Venezuelan basin
VDB
a
90°W
60°W
Cuba
Puerto Rico
Jamaica
Hispaniola
18°N
Central America
South America
Galapagos Is.
0°N
-73.54W- 18.66N
-70.94W- 18.66N
Plantain Garden-Enriquillo Fault
PORT AU PRINCE
LA DESCUBIERTA
Massif de la Hotte
Chaîne de la Selle
JIMAN
Sierra de Bahoruco
BARAHONA
LA CIENAGA
HAITI
PEDERNALES
REPUBLICA DOMINICANA
Isla Beata
(c)
b
0
40 km
-73.54W- 17.54N
-70.94W- 17.54N
PUNTA CEMINCHI
LA SALINA
POLO
OVIEDO
BARAHONA
ENRIQUILLO
LA CIENAGA
5970II-JE9620
5970II-JE9621
5970II-JE9625
5970II-JE9626
5970II-MJ9111
5969I-JE9623
5969I-JE9622
5970II-JE9623
5970II-JE9624
5970II-JE9619
5970II-MJ9150
C
Sample location
Quaternary (undifferenciated)
La Isabela Fm.Reef limestones Pleistocene-Holocene
Reef and shallow limestones Pliocene-Pleistocene
Barahona and Enriquillo units Middle Miocene-Pleistocene
Las Mercedes Fm (Pedernales Group) Miocene
Quemados unit (Pedernales G.) Upper Oligoc.-lower Miocene
Trudillé-Aceitillar Unit Eocene-Oligocene
Neiba Fm Upper Eocene-lower Miocene
Dumisseau Fm Late Cretaceous

Figure 1

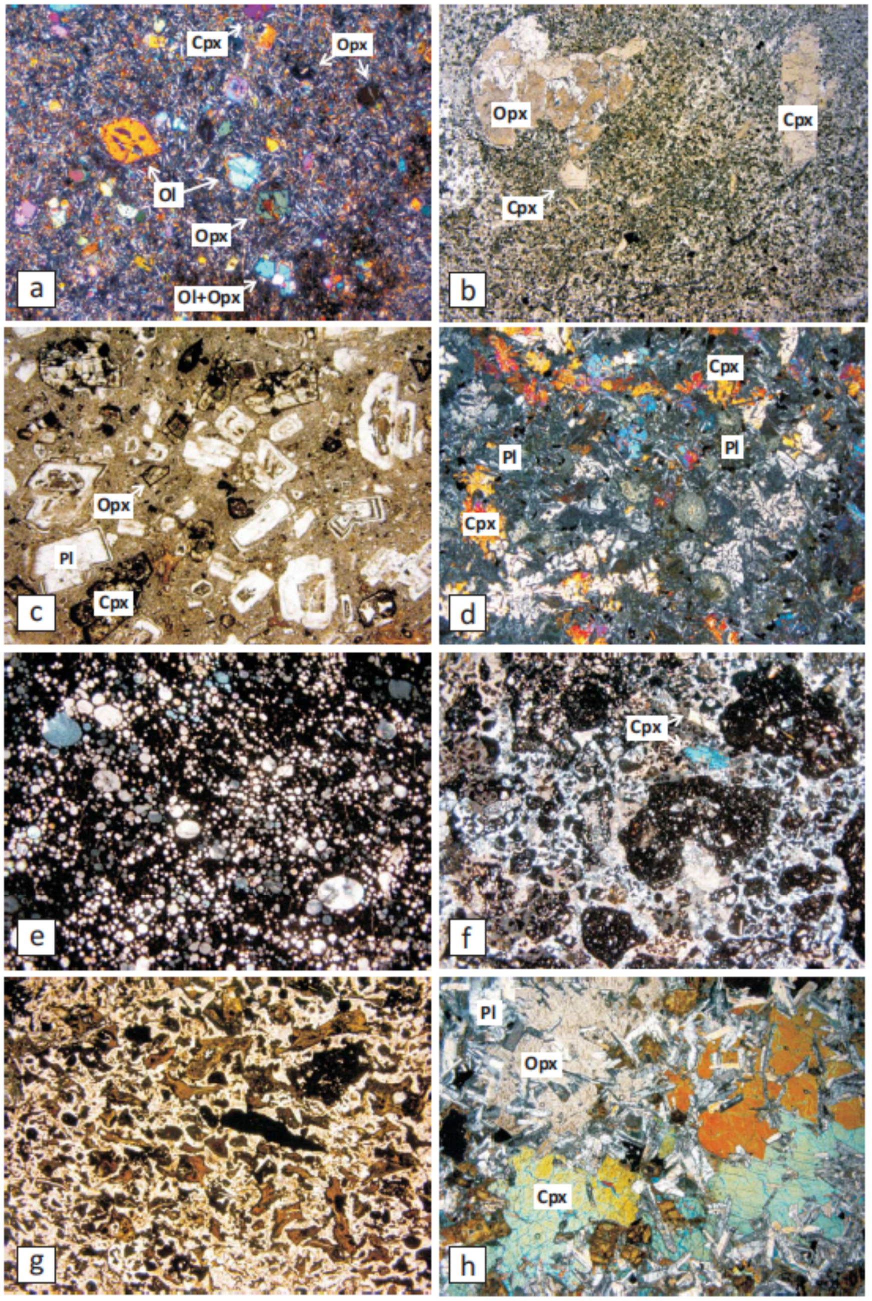
Cpx
Opx
Ol
Opx
Ol+Opx
a
Opx
Cpx
Cpx
b
Opx
Pl
Cpx
c
Cpx
Pl
Pl
Cpx
d
e
Cpx
f
g
Pl
Opx
Cpx
h

Figure 2

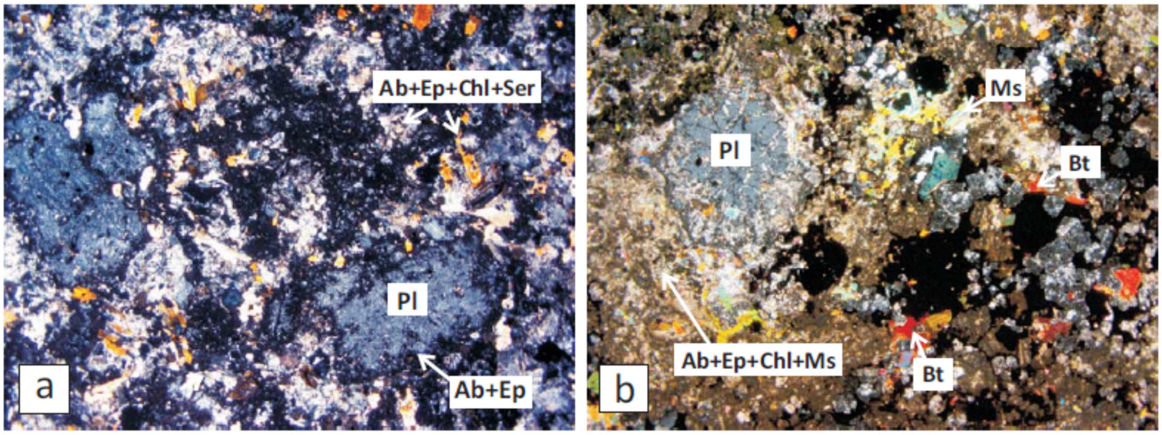

Figure 3

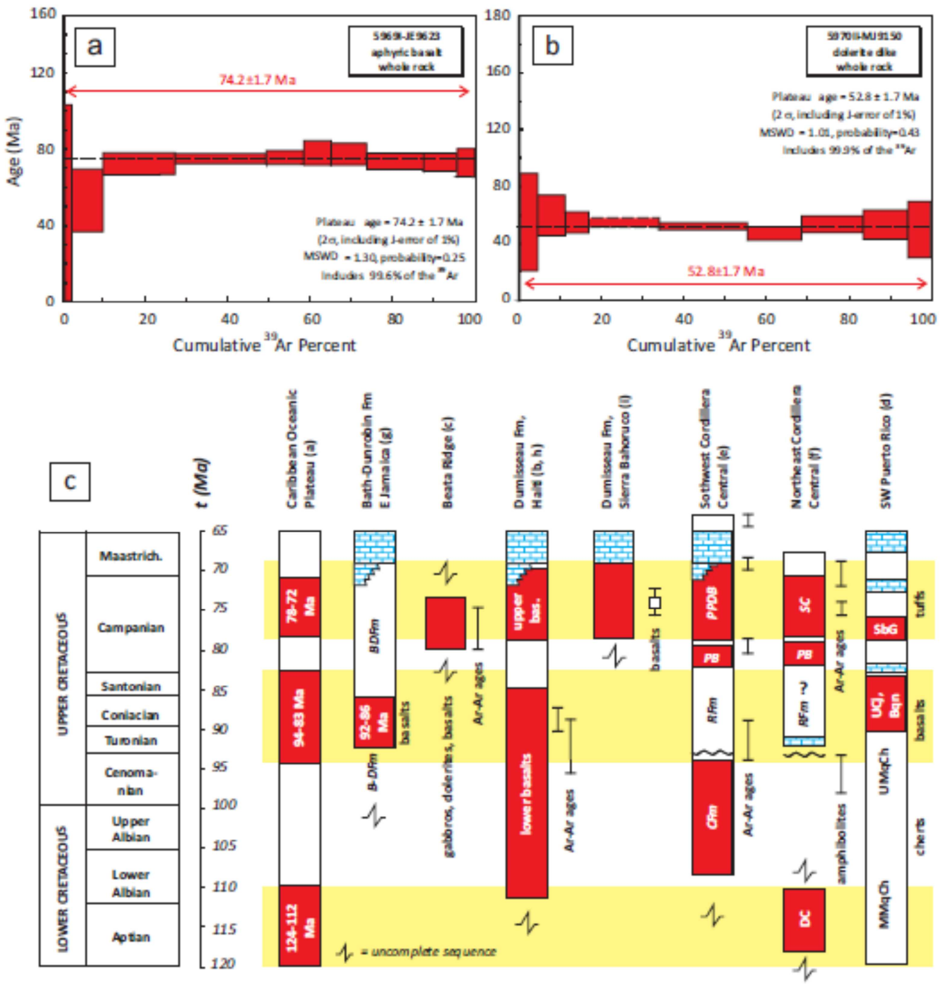
a
5969I-JE9623
aphyric basalt
whole rock
74.2±1.7 Ma
Plateau age = 74.2 ± 1.7 Ma
(2σ, including J-error of 1%)
MSWD = 1.30, probability=0.25
Includes 99.6% of the 39Ar
Age (Ma)
0
40
80
120
160
0
20
40
60
80
100
Cumulative 39Ar Percent
b
59708-MJ9150
dolerite dike
whole rock
Plateau age = 52.8 ± 1.7 Ma
(2σ, including J-error of 1%)
MSWD = 1.01, probability=0.43
Includes 99.9% of the 39Ar
52.8±1.7 Ma
0
40
80
120
160
180
0
20
40
60
80
100
Cumulative 39Ar Percent
c
t (Ma)
UPPER CRETACEOUS
LOWER CRETACEOUS
Maastrich.
Campanian
Santonian
Coniacian
Turonian
Cenomanian
Upper Albian
Lower Albian
Aptian
65
70
75
80
85
90
95
100
105
110
115
120
Caribbean Oceanic Plateau (a)
Bath-Dunrobin Fm E Jamaica (g)
Beata Ridge (c)
Dumisseau Fm, Haiti (b, h)
Dumisseau Fm, Sierra Bahoruco (i)
Sothwest Cordillera Central (e)
Northeast Cordillera Central (f)
SW Puerto Rico (d)
78-72 Ma
94-83 Ma
124-112 Ma
BDFm
92-86 Ma
basalts
B-DFm
gabbros, dolerites, basalts
Ar-Ar ages
upper bas.
lower basalts
Ar-Ar ages
basalts
PPDB
PB
RFm
CFm
Ar-Ar ages
SC
PB
RFm ?
DC
Ar-Ar ages
amphibolites
SbG
UCJ, Bqn
UMqCh
MMqCh
tuffs
basalts
cherts
= uncomplete sequence

Figure 4

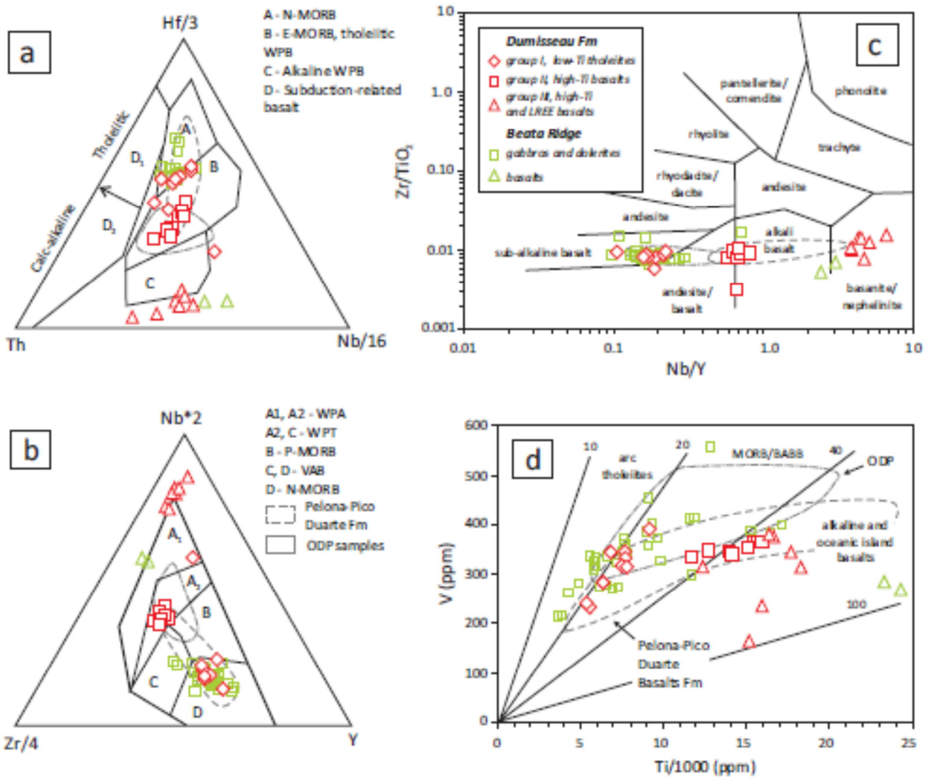
a
Hf/3
Th
Nb/16
A - N-MORB
B - E-MORB, tholeiitic WPB
C - Alkaline WPB
D - Subduction-related basalt
Tholeiitic
Calc-alkaline
D_1
D_2
A
B
C
c
Zr/TiO$_2$
Nb/Y
10
1.0
0.10
0.01
0.001
0.01
0.1
1.0
10
Dumisseau Fm
group I, low-Ti tholeiites
group II, high-Ti basalts
group III, high-Ti and LREE basalts
Beata Ridge
gabbros and dolerites
basalts
pantellerite/comendite
phonolite
rhyolite
trachyte
rhyodacite/dacite
andesite
andesite
alkali basalt
sub-alkaline basalt
andesite/basalt
basanite/nephelinite
b
Nb*2
Zr/4
Y
A1, A2 - WPA
A2, C - WPT
B - P-MORB
C, D - VAB
D - N-MORB
Pelona-Pico Duarte Fm
ODP samples
A_1
A_2
B
C
D
d
V (ppm)
Ti/1000 (ppm)
600
500
400
300
200
100
0
0
5
10
15
20
25
10
20
40
100
arc tholeiites
MORB/BABB
ODP
alkaline and oceanic island basalts
Pelona-Pico Duarte Basalts Fm

Figure 5

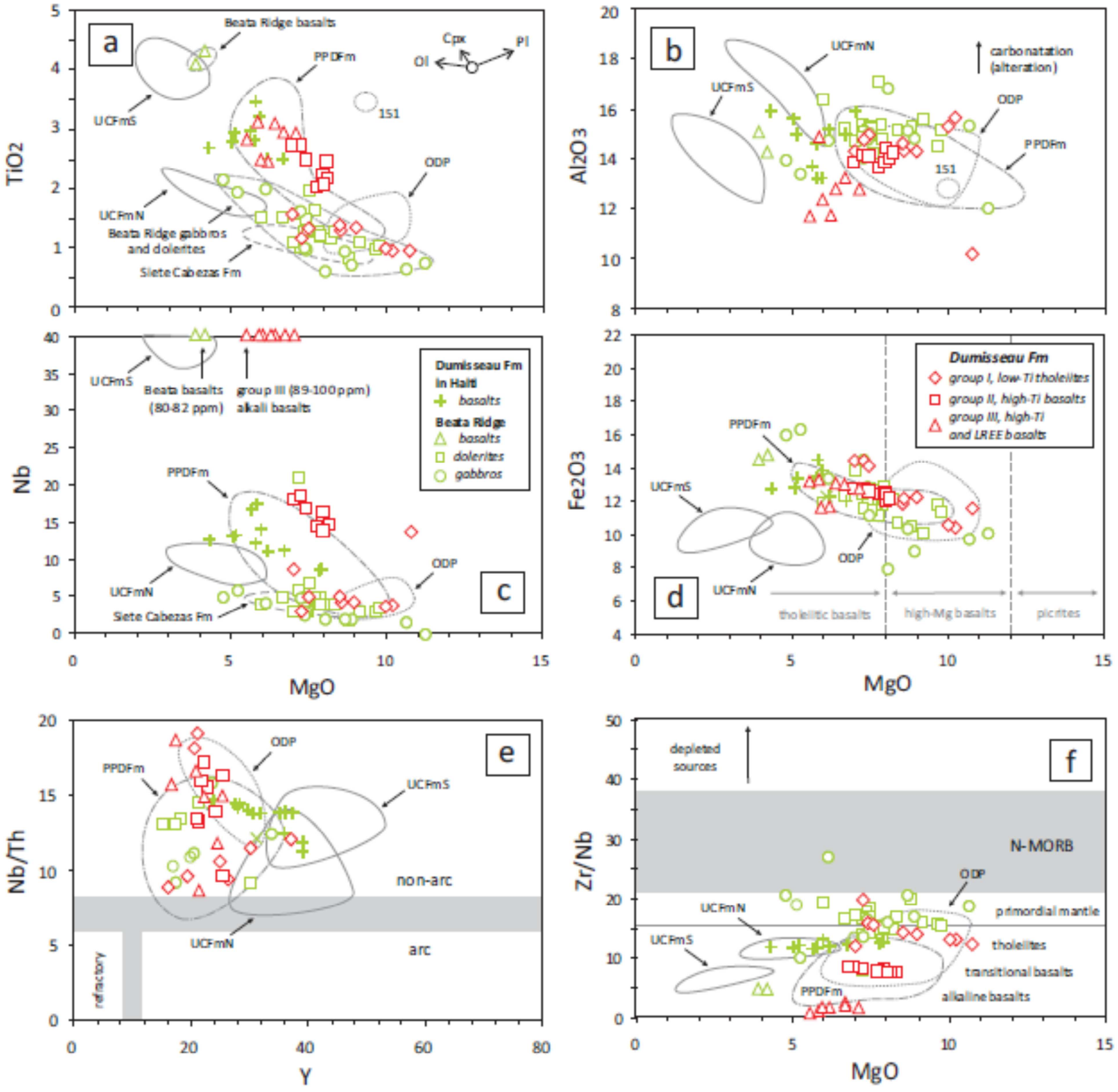
a
TiO2
Beata Ridge basalts
PPDFm
Cpx
Ol
Pl
151
UCFmS
ODP
UCFmN
Beata Ridge gabbros and dolerites
Siete Cabezas Fm
b
Al2O3
UCFmN
carbonatation (alteration)
UCFmS
ODP
PPDFm
151
c
Nb
UCFmS
Beata basalts (80-82 ppm)
group III (89-100 ppm) alkali basalts
Dumisseau Fm in Haiti
basalts
Beata Ridge
basalts
dolerites
gabbros
PPDFm
UCFmN
Siete Cabezas Fm
ODP
MgO
d
Fe2O3
Dumisseau Fm
group I, low-Ti tholeiites
group II, high-Ti basalts
group III, high-Ti and LREE basalts
PPDFm
UCFmS
ODP
UCFmN
tholeiitic basalts
high-Mg basalts
picrites
MgO
e
Nb/Th
PPDFm
ODP
UCFmS
non-arc
arc
UCFmN
refractory
Y
f
Zr/Nb
depleted sources
N-MORB
ODP
UCFmN
primordial mantle
UCFmS
tholeiites
PPDFm
transitional basalts
alkaline basalts
MgO

Figure 6

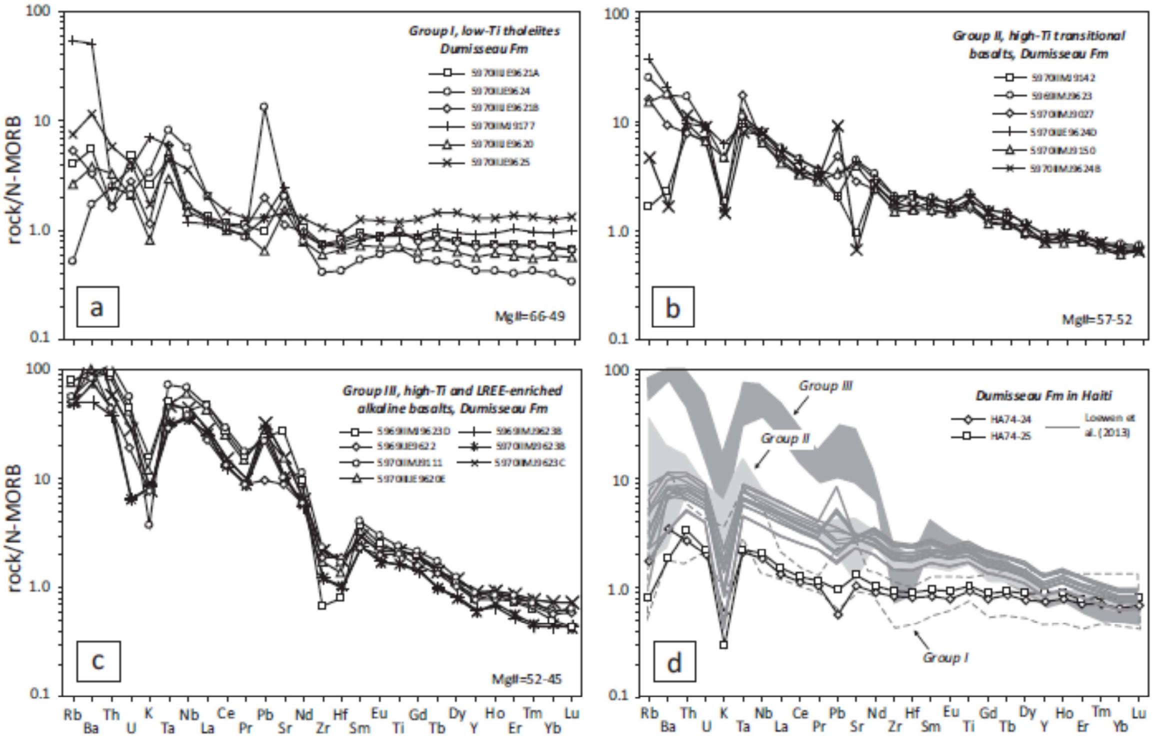
Group I, low-Ti tholeiites
Dumisseau Fm
5970IIUE9621A
5970IIUE9624
5970IIUE9621B
5970IIMJ9177
5970IIUE9620
5970IIUE9625
a
MgII=66-49
Group II, high-Ti transitional
basalts, Dumisseau Fm
5970IIMJ9142
5969IIMJ9623
5970IIMJ9027
5970IIUE9624D
5970IIMJ9150
5970IIMJ9624B
b
MgII=57-52
Group III, high-Ti and LREE-enriched
alkaline basalts, Dumisseau Fm
5969IIMJ9623D
5969IIUE9622
5970IIMJ9111
5970IIUE9620E
5969IIMJ9623B
5970IIMJ9623B
5970IIMJ9623C
c
MgII=52-45
Dumisseau Fm in Haiti
HA74-24
HA74-25
Loewen et al. (2013)
Group III
Group II
Group I
d
rock/N-MORB
100
10
1.0
0.1
Rb Ba Th U K Ta Nb La Ce Pr Pb Sr Nd Zr Hf Sm Eu Ti Gd Tb Dy Y Ho Er Tm Yb Lu

Figure 7

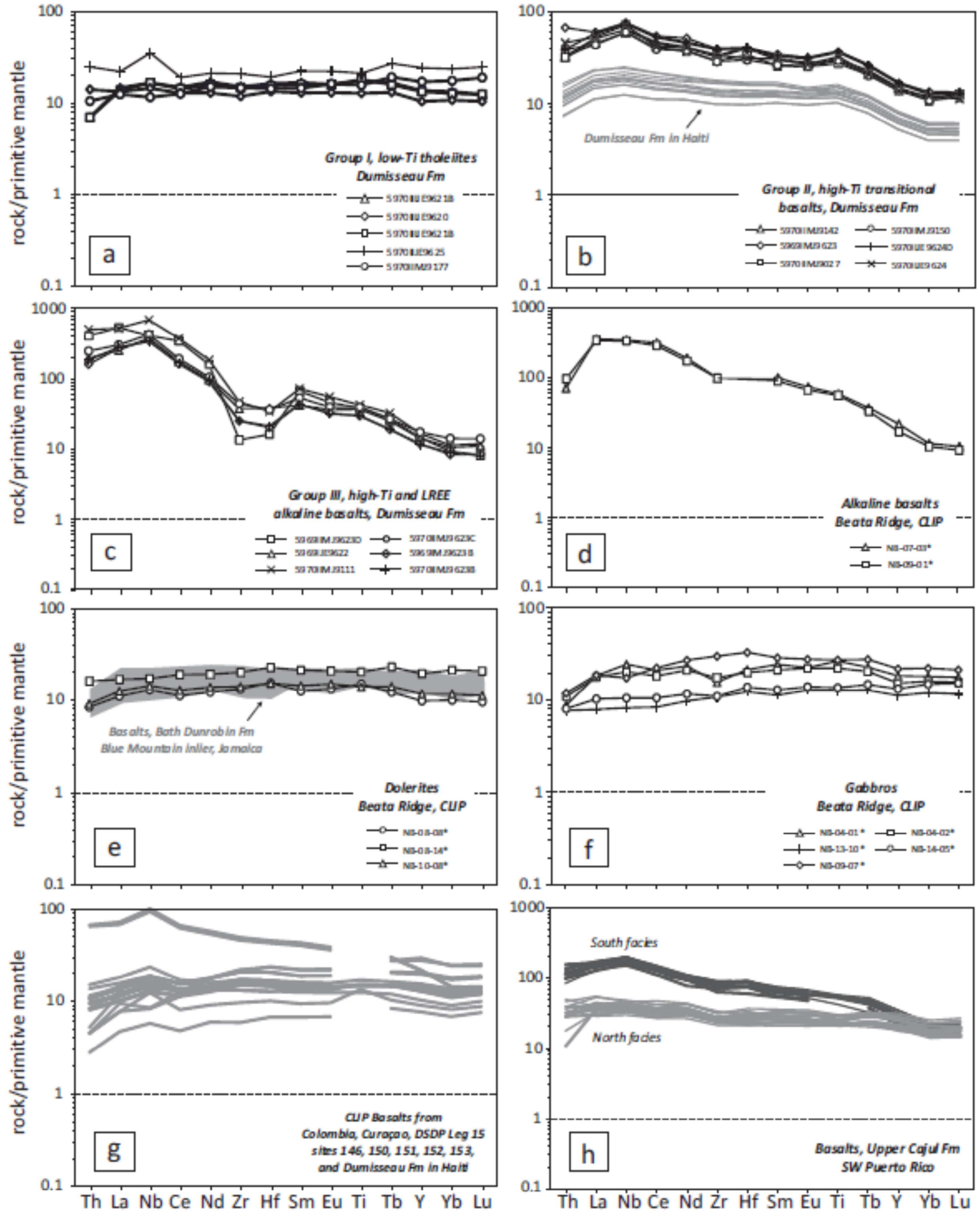
100
10
1
0.1
rock/primitive mantle
Group I, low-Ti tholeiites
Dumisseau Fm
5970IIJE96218
5970IIJE9620
5970IIJE96218
5970IIJE9625
5970IIMJ9177
a
Dumisseau Fm in Haiti
Group II, high-Ti transitional
basalts, Dumisseau Fm
5970IIMJ9142
5970IIMJ9150
5969IIMJ9623
5970IIJE9624D
5970IIMJ9027
5970IIJE9624
b
1000
Group III, high-Ti and LREE
alkaline basalts, Dumisseau Fm
5969IIMJ9623D
5970IIMJ9623C
5969IIJE9622
5969IIMJ9623B
5970IIMJ9111
5970IIMJ9623B
c
Alkaline basalts
Beata Ridge, CLIP
NB-07-03*
NB-09-01*
d
Basalts, Bath Dunrobin Fm
Blue Mountain inlier, Jamaica
Dolerites
Beata Ridge, CLIP
NB-08-08*
NB-08-14*
NB-10-08*
e
Gabbros
Beata Ridge, CLIP
NB-04-01*
NB-04-02*
NB-13-10*
NB-14-05*
NB-09-07*
f
CLIP Basalts from
Colombia, Curaçao, DSDP Leg 15
sites 146, 150, 151, 152, 153,
and Dumisseau Fm in Haiti
g
South facies
North facies
Basalts, Upper Cajul Fm
SW Puerto Rico
h
Th La Nb Ce Nd Zr Hf Sm Eu Ti Tb Y Yb Lu
Th La Nb Ce Nd Zr Hf Sm Eu Ti Tb Y Yb Lu

Figure 8

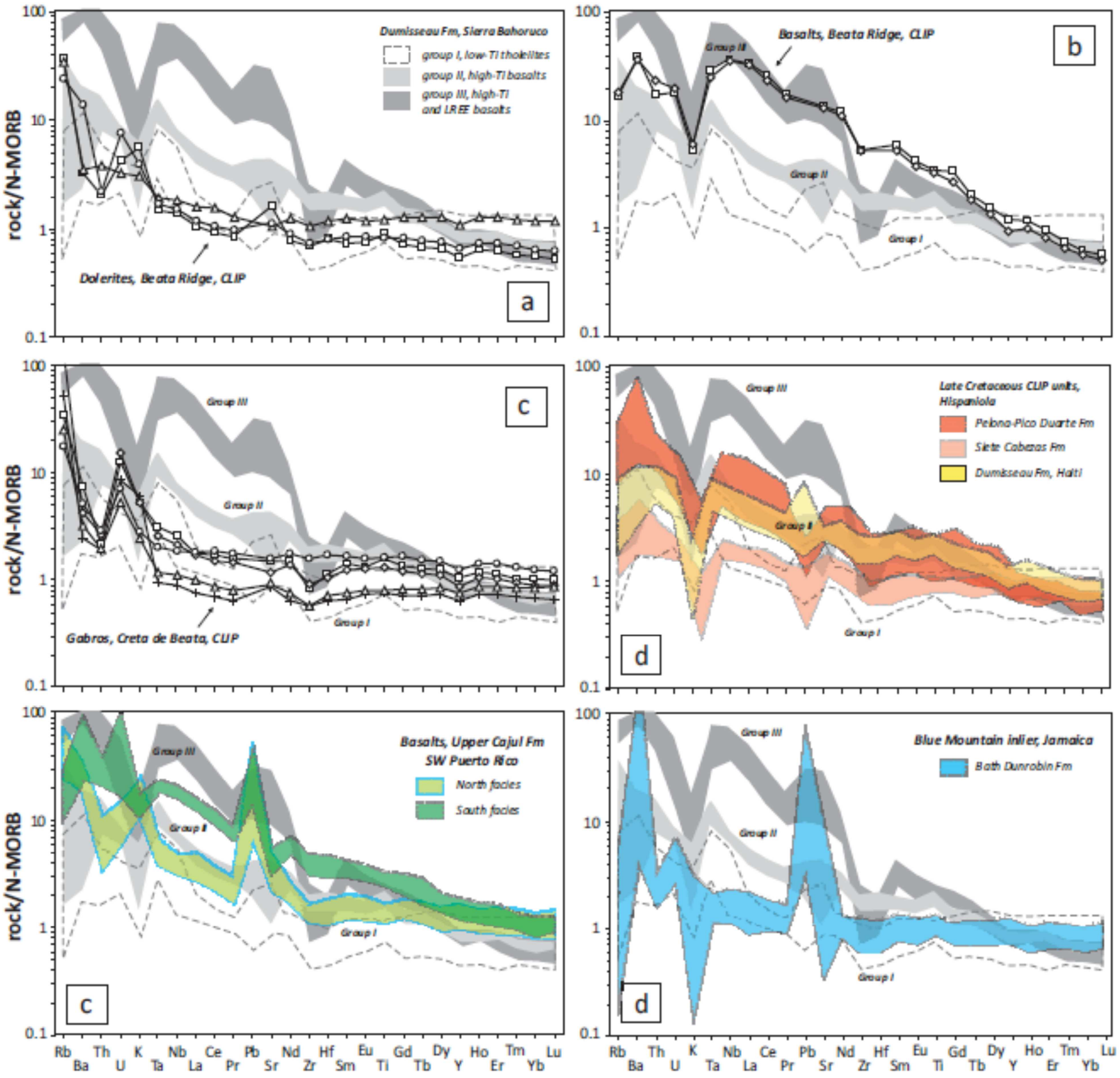
rock/N-MORB
100
10
1
0.1
Dumisseau Fm, Sierra Bahoruco
group I, low-Ti tholeiites
group II, high-Ti basalts
group III, high-Ti and LREE basalts
Dolerites, Beata Ridge, CLIP
a
Basalts, Beata Ridge, CLIP
Group III
Group II
Group I
b
Gabros, Creta de Beata, CLIP
c
Late Cretaceous CLIP units, Hispaniola
Pelona-Pico Duarte Fm
Siete Cabezas Fm
Dumisseau Fm, Haiti
d
Basalts, Upper Cajul Fm SW Puerto Rico
North facies
South facies
c
Blue Mountain inlier, Jamaica
Bath Dunrobin Fm
d
Rb
Ba
Th
U
K
Ta
Nb
La
Ce
Pr
Pb
Sr
Nd
Zr
Hf
Sm
Eu
Ti
Gd
Tb
Dy
Y
Ho
Er
Tm
Yb
Lu

Figure 9

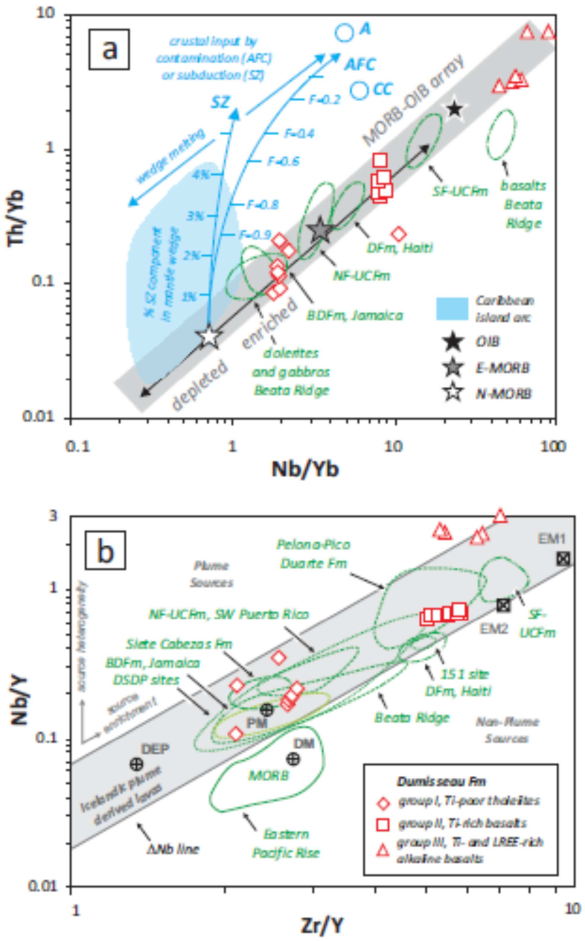
a
10
1
0.1
0.01
Th/Yb
0.1
1
10
100
Nb/Yb
crustal input by contamination (AFC) or subduction (SZ)
A
AFC
CC
SZ
F=0.2
F=0.4
F=0.6
F=0.8
F=0.9
wedge melting
4%
3%
2%
1%
% SZ component in mantle wedge
MORB-OIB array
SF-UCFm
basalts Beata Ridge
DFm, Haiti
NF-UCFm
BDFm, Jamaica
enriched
depleted
dolerites and gabbros Beata Ridge
Caribbean island arc
OIB
E-MORB
N-MORB
b
3
1
0.1
0.01
Nb/Y
1
10
Zr/Y
Plume Sources
Pelona-Pico Duarte Fm
EM1
EM2
SF-UCFm
NF-UCFm, SW Puerto Rico
Siete Cabezas Fm
BDFm, Jamaica
DSDP sites
source heterogeneity
source enrichment
PM
DM
DEP
151 site
DFm, Haiti
Beata Ridge
Non-Plume Sources
MORB
Icelandic plume derived lavas
ΔNb line
Eastern Pacific Rise
Dumisseau Fm
group I, Ti-poor tholeiites
group II, Ti-rich basalts
group III, Ti- and LREE-rich alkaline basalts

Figure 10

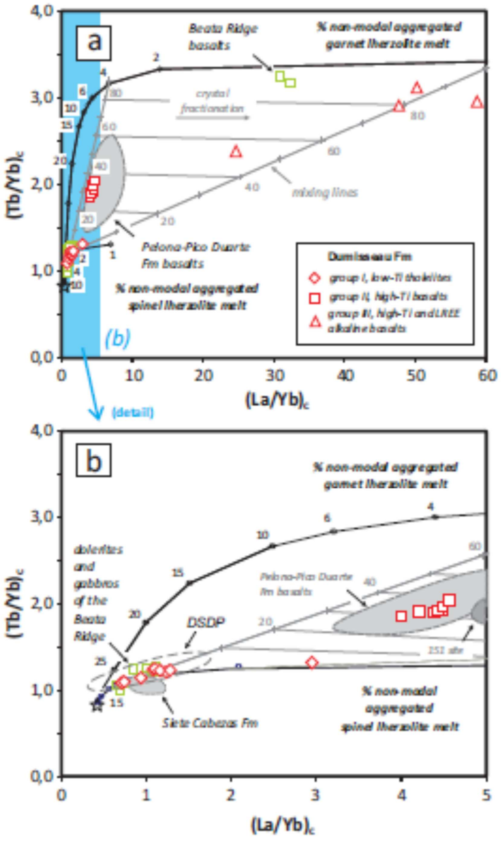
a
Beata Ridge basalts
% non-modal aggregated garnet lherzolite melt
crystal fractionation
mixing lines
Pelona-Pico Duarte Fm basalts
% non-modal aggregated spinel lherzolite melt
Dumisseau Fm
◇ group I, low-Ti tholeiites
□ group II, high-Ti basalts
△ group III, high-Ti and LREE alkaline basalts
(b)
(detail)
(Tb/Yb)c
(La/Yb)c
0,0
1,0
2,0
3,0
4,0
0
10
20
30
40
50
60
b
% non-modal aggregated garnet lherzolite melt
dolerites and gabbros of the Beata Ridge
DSDP
Pelona-Pico Duarte Fm basalts
151 site
Siete Cabezas Fm
% non-modal aggregated spinel lherzolite melt
(Tb/Yb)c
(La/Yb)c
0,0
1,0
2,0
3,0
4,0
0
1
2
3
4
5

Figure 11

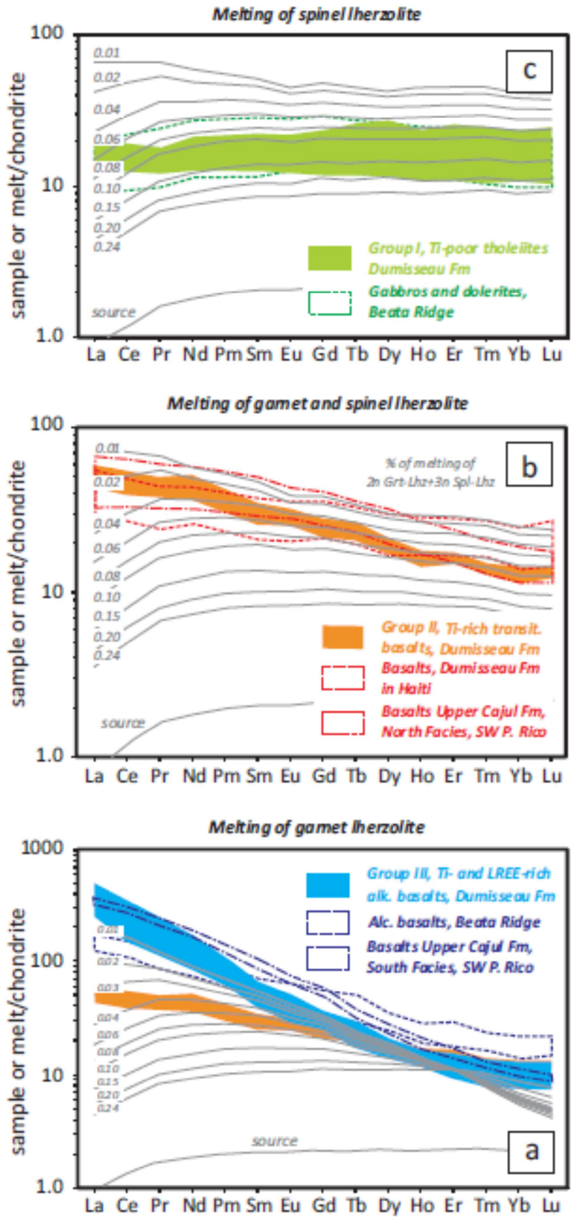
Melting of spinel lherzolite
c
0.01
0.02
0.04
0.06
0.08
0.10
0.15
0.20
0.24
source
Group I, Ti-poor tholeiites Dumisseau Fm
Gabbros and dolerites, Beata Ridge
Melting of garnet and spinel lherzolite
b
% of melting of 2n Grt-Lhz+3n Spl-Lhz
Group II, Ti-rich transit. basalts, Dumisseau Fm
Basalts, Dumisseau Fm in Haiti
Basalts Upper Cajul Fm, North Facies, SW P. Rico
Melting of garnet lherzolite
a
Group III, Ti- and LREE-rich alk. basalts, Dumisseau Fm
Alc. basalts, Beata Ridge
Basalts Upper Cajul Fm, South Facies, SW P. Rico
sample or melt/chondrite
1000
100
10
1.0
La Ce Pr Nd Pm Sm Eu Gd Tb Dy Ho Er Tm Yb Lu

Figure 12

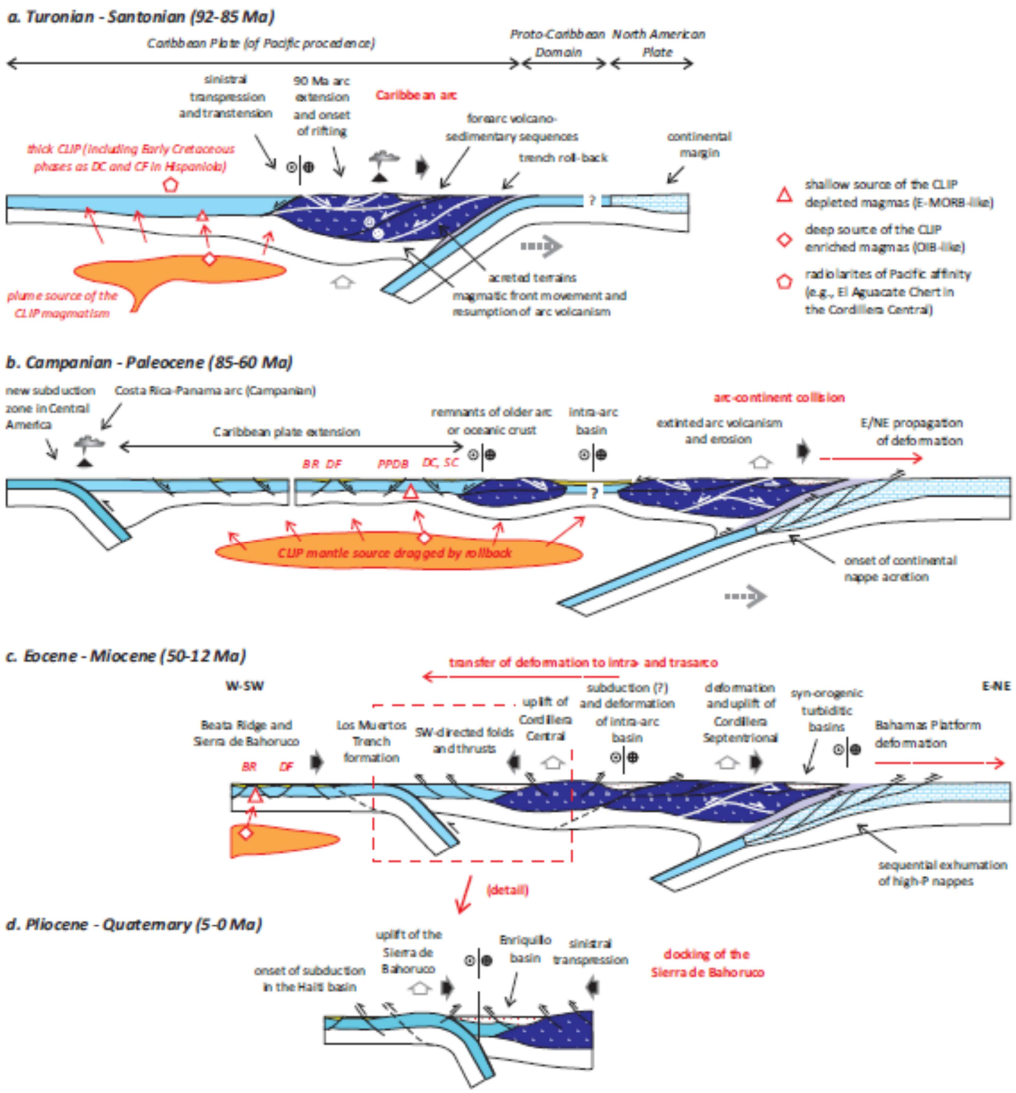
a. Turonian - Santonian (92-85 Ma)
Caribbean Plate (of Pacific procedence)
Proto-Caribbean Domain
North American Plate
sinistral transpression and transtension
90 Ma arc extension and onset of rifting
Caribbean arc
forearc volcano-sedimentary sequences
trench roll-back
continental margin
thick CLIP (including Early Cretaceous phases as DC and CF in Hispaniola)
?
plume source of the CLIP magmatism
acreted terrains
magmatic front movement and resumption of arc volcanism
△ shallow source of the CLIP depleted magmas (E-MORB-like)
◇ deep source of the CLIP enriched magmas (OIB-like)
⬠ radiolarites of Pacific affinity (e.g., El Aguacate Chert in the Cordillera Central)
b. Campanian - Paleocene (85-60 Ma)
new subduction zone in Central America
Costa Rica-Panama arc (Campanian)
Caribbean plate extension
remnants of older arc or oceanic crust
intra-arc basin
arc-continent collision
extinted arc volcanism and erosion
E/NE propagation of deformation
BR DF
PPDB
DC, SC
?
CLIP mantle source dragged by rollback
onset of continental nappe acretion
c. Eocene - Miocene (50-12 Ma)
transfer of deformation to intra- and trasarco
W-SW
E-NE
Beata Ridge and Sierra de Bahoruco
Los Muertos Trench formation
SW-directed folds and thrusts
uplift of Cordillera Central
subduction (?) and deformation of intra-arc basin
deformation and uplift of Cordillera Septentrional
syn-orogenic turbiditic basins
Bahamas Platform deformation
BR
DF
sequential exhumation of high-P nappes
(detail)
d. Pliocene - Quaternary (5-0 Ma)
onset of subduction in the Haiti basin
uplift of the Sierra de Bahoruco
Enriquillo basin
sinistral transpression
docking of the Sierra de Bahoruco

Figure 13

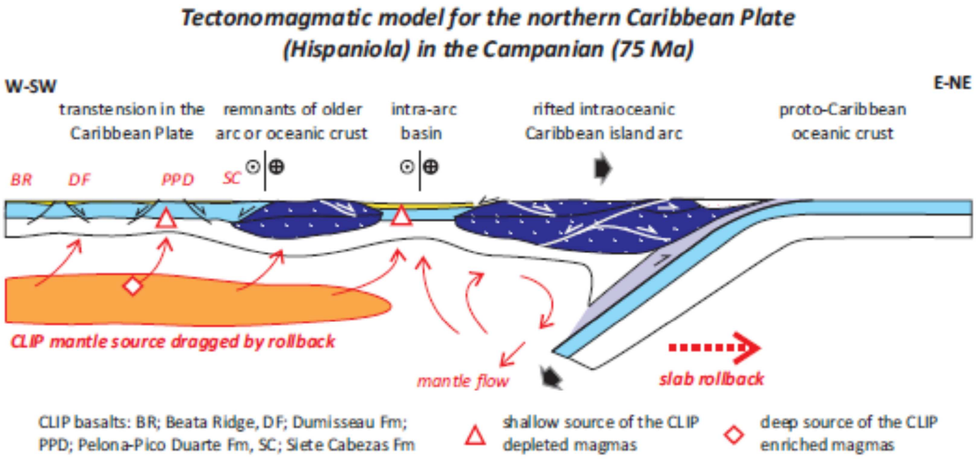

Graphical abstract

Highlights

The basaltic volcanism of the Dumisseau Fm is plume-related

It is composed of tholeiites, transitional and alkaline basalts.

It represents an emerged fragment of the CLIP